DMD Fast Forward. Published on October 1, 2012 as doi:10.1124/dmd.112.048017

DMD #48017

Autoinhibition of CYP3A4 Leads to Major Role of CYP2C8 in Imatinib Metabolism: Variability in CYP2C8 Activity May Alter Plasma Concentrations and Response

Anne M. Filppula, Mikko Neuvonen, Jouko Laitila, Pertti J. Neuvonen, and Janne T. Backman

Department of Clinical Pharmacology, University of Helsinki, Helsinki, Finland *(A.M.F., M.N., J.L., P.J.N., J.T.B.)* and HUSLAB, Helsinki University Central Hospital, Helsinki, Finland *(P.J.N., J.T.B.)*

DMD Fast Forward. Published on October 1, 2012 as DOI: 10.1124/dmd.112.048017
This article has not been copyedited and formatted. The final version may differ from this version.

Running Title Page

Running title: Major role for CYP2C8 in imatinib metabolism

Correspondence: Prof. Janne T. Backman

Department of Clinical Pharmacology

University of Helsinki and HUSLAB, Helsinki University Central Hospital

P.O. Box 705, FI-00029 HUS

FINLAND

Phone: +358 (0)50 428 0997

Fax: +358 (0)9 471 74039

E-mail: janne.backman@helsinki.fi

Text pages: 16

Tables: 1 (plus 8 supplementary tables)

Figures: 5 (plus 2 supplementary figures)

References: 53

Words in Abstract: 250

Words in Introduction: 668

Words in Discussion: 1,569

Abbreviations: AUC, area under the concentration-time curve; C_{max}, peak concentration; CL_H, hepatic clearance; CL_{int}, intrinsic clearance; DDC, diethyldithiocarbamate; GEM-G, gemfibrozil 1-O-*β* glucuronide; HLM, human liver microsomes; ISEF, intersystem extrapolation factor; 8-M-P, 8-methoxy-psoralen; MBI, mechanism-based inhibition; N-DMI, N-desmethylimatinib; P450, cytochrome P450; PBPK, physiologically-based pharmacokinetic.

Abstract

Recent data suggest that the role of CYP3A4 in imatinib metabolism is smaller than presumed. This study aimed to evaluate the quantitative importance of different cytochrome P450 (P450) enzymes in imatinib pharmacokinetics. First, the metabolism of imatinib was investigated using recombinant P450 enzymes and human liver microsomes with P450 isoform-selective inhibitors. Thereafter, an *in silico* model for imatinib was constructed to perform pharmacokinetic simulations to assess the roles of P450 enzymes in imatinib elimination at clinically used imatinib doses. *In vitro*, CYP2C8 inhibitors and CYP3A4 inhibitors inhibited the depletion of 0.1 µM imatinib by 45% and 80%, respectively, and the formation of the main metabolite of imatinib, N-desmethylimatinib, by >50%. Likewise, recombinant CYP2C8 and CYP3A4 metabolized imatinib extensively, whereas other isoforms had minor effect on imatinib concentrations. In the beginning of imatinib treatment, the fractions of its hepatic clearance mediated by CYP2C8 and CYP3A4 were predicted to approximate 40% and 60%, respectively. During long-term treatment with imatinib 400 mg once or twice daily, up to 65% or 75% of its hepatic elimination was predicted to occur via CYP2C8, and only about 35% or 25% by CYP3A4, due to dose- and time-dependent autoinactivation of CYP3A4 by imatinib. Thus, although CYP2C8 and CYP3A4 are the main enzymes in imatinib metabolism *in vitro, in silico* predictions indicate that imatinib inhibits its own CYP3A4-mediated metabolism, assigning a key role for CYP2C8. During multiple dosing, pharmacogenetic polymorphisms and drug interactions affecting CYP2C8 activity may cause marked interindividual variation in the exposure and response to imatinib.

DMD Fast Forward. Published on October 1, 2012 as DOI: 10.1124/dmd.112.048017
This article has not been copyedited and formatted. The final version may differ from this version.

Introduction

The tyrosine kinase inhibitor imatinib (Gleevec, Glivec) has revolutionized the treatment of chronic myelogenous leukemia, advanced gastrointestinal stromal tumours and certain other hematologic and oncologic malignancies (Kovacsovics and Maziarz, 2006; Duffaud and Le Cesne, 2009; Stegmeier et al., 2010). The success of imatinib is mostly due to its excellent efficacy but also because of its tolerability. Both the clinical response and adverse effects of imatinib are associated with its plasma levels, which exhibit a wide interindividual variability, and therapeutic drug monitoring has been recommended for imatinib (Peng et al., 2004b; Picard et al., 2007; Teng et al., 2012). According to clinical studies, achieving and maintaining an imatinib plasma level of >1,000 ng/ml is associated with better response rates, whereas doses of >600 mg daily have been linked to an increased risk of adverse events (Picard et al., 2007; Larson et al., 2008; Takahashi et al., 2010; Teng et al., 2012). Accordingly, it is important to know the potential sources of variability in imatinib pharmacokinetics.

Imatinib has a rapid absorption, complete oral bioavailability (>97%) and a terminal elimination half-life of 18-20 h (Peng et al., 2004a; Peng et al., 2004b), making it suitable for once or twice daily oral administration. Imatinib undergoes extensive hepatic metabolism and its metabolites are excreted principally into feces and, to a lesser extent, into urine (http://www.accessdata.fda.gov/drugsatfda_docs/nda/2001/21335_Gleevec.cfm)(Gschwind et al., 2005). Following a single oral dose, parent imatinib accounts for approximately 70% of the drug concentration in plasma, whereas its pharmacologically active main metabolite N-desmethylimatinib (N-DMI; CGP74588) accounts for a respective 10% (Gschwind et al., 2005; Peng et al., 2005)(Supplementary Fig. S1). Several other, less important metabolites have been identified, including both oxidative and glucuronide conjugated metabolites of imatinib and N-DMI (Gschwind et al., 2005; Rochat et al., 2008).

According to imatinib product information, imatinib metabolism is mainly mediated by cytochrome P450 3A4 (http://www.ema.europa.eu/docs/en_GB/document_library/EPAR_-_Product_Information/human/000406/WC500022207.pdf, http://www.accessdata.fda.gov/drugsatfda_docs/nda/2001/21335_Gleevec.cfm)(Rochat et al., 2008; Nebot et al., 2010). Recently, however, we demonstrated that imatinib is a potent mechanism-based inhibitor of this enzyme *in vitro*, and clinically relevant imatinib concentrations were predicted to cause

DMD Fast Forward. Published on October 1, 2012 as DOI: 10.1124/dmd.112.048017
This article has not been copyedited and formatted. The final version may differ from this version.

up to 90% inhibition of hepatic CYP3A4 activity (Filppula et al., 2012). These findings suggest that imatinib can affect its own CYP3A4-mediated metabolism, which may reduce the significance of this enzyme in its elimination *in vivo*. In fact, strong CYP3A4 inhibitors have had only little effect on imatinib pharmacokinetics in the beginning of therapy, and no effect at all during long-term treatment. In healthy volunteers, the CYP3A4-inhibiting antifungal agent ketoconazole increased the area under the plasma concentration-time curve (AUC) of imatinib after single dose administration by 40% only (Dutreix et al., 2004), and in patients steady-state imatinib pharmacokinetics were unchanged by ritonavir, a CYP3A4-inhibiting antiretroviral drug (van Erp et al., 2007).

Recent *in vitro* data suggest that in addition to CYP3A4, also CYP2C8 contributes to the formation of N-DMI (Nebot et al., 2010); recombinant human CYP2C8 catalyzed the N-demethylation of imatinib at a much higher rate than did CYP3A4 and CYP3A5. However, the significance of CYP2C8 to the human metabolism of imatinib is difficult to estimate because the recombinant CYP2C8 and CYP3A5 enzymes used in this previous study were produced in insect cells, whereas the recombinant CYP3A4 originated from human lymphoblastoid cells, which typically show a several-fold lower activity than enzymes from insect cells. Furthermore, because the contributions of P450 enzymes to the overall metabolism of imatinib, including both its N-demethylation and other metabolic pathways, and to the further metabolism of N-DMI were not investigated, the clinical significance of the previous *in vitro* results cannot be estimated.

Using recombinant human P450 enzymes, human liver microsomes (HLM) and chemical P450 inhibitors, we carefully examined the contributions of different P450 enzymes, particularly those of CYP2C8 and CYP3A4, to the main metabolic pathway of imatinib and the further metabolism of N-DMI. Furthermore, in order to translate our laboratory findings to clinical relevance, we used our data for pharmacokinetic and drug-drug interaction simulations by constructing a physiologically-based model of imatinib pharmacokinetics, incorporating the time-dependent inhibitory effect of imatinib on its own CYP3A4-mediated metabolism.

Materials and Methods

In vitro study

Chemicals and Microsomes.

Imatinib mesilate (mesylate salt), clopidogrel and montelukast were purchased from Sequoia Research Products Ltd. (Pangbourne, UK), N-DMI and N-DMI-d8 from SynFine Research Inc. (Richmond Hill, ON, Canada), imatinib-d8 mesilate and gemfibrozil 1-*O*-β glucuronide (GEM-G) from Toronto Research Chemicals Inc. (North York, ON, CAN), diethyldithiocarbamate (DDC), furafylline, 8-methoxy-psoralen (8-M-P), omeprazole, quinidine, sulfaphenazole, troleandomycin, and β-NADPH from Sigma-Aldrich (St. Louis, MO, USA), and ketoconazole from Janssen Biotech (Olen, Belgium). Pooled HLM and Supersomes™ (human recombinant P450 enzymes and control supersomes) were obtained from BD Biosciences (Woburn, MA, USA). Other chemicals were from Merck (Darmstadt, Germany).

Incubation conditions.

Incubations were carried out in a shaking water bath (37°C) in triplicates (mean value used as the result). The incubations contained HLM or recombinant P450 enzymes in 0.1 M sodium phosphate buffer (pH 7.4). To keep the possible nonspecific binding of imatinib equal in the experiments and to enable precise comparisons of results with different P450 isoforms, an equal protein concentration (0.5 mg/ml; unless otherwise indicated) was used in parallel experiments (resulting in variable P450 contents in recombinant isoform studies). Except for inhibition studies, experiments were started by premixing imatinib for 3 min with microsomes, followed by addition of β-NADPH (final concentration 1 mM) to initiate the reaction. In competitive inhibition studies, imatinib and inhibitor or buffer control were (simultaneously) premixed with HLM for 3 min before β-NADPH addition. In mechanism-based inhibition (MBI) studies, except for that with GEM-G, the inhibitor or buffer control was first premixed with HLM for 3 min before addition of β-NADPH. After a 15-min preincubation, including β-NADPH, imatinib was added to start the reaction. Inhibition by GEM-G (60 µM) was investigated by premixing it with 10 mg/ml HLM in buffer. After addition of β-NADPH, the solution was preincubated for 20 min. An aliquot of 25 µl was then moved to another tube containing β-NADPH in buffer, and imatinib was immediately added to start the reaction in a final incubation volume of 0.5 ml. Thus, the protein and

inhibitor concentrations had been diluted 20-fold to avoid possible competitive inhibition of other enzymes by the inhibitor.

After incubation, reactions were stopped by moving incubation mixture to ACN containing the internal standards imatinib-d8 and N-DMI-d8, 10% MeOH and 0.1% HCOOH, diluting the incubation mixture 3-fold. Samples were immediately vortexed, put on ice for at least 10 minutes, and vortexed further two times before centrifugation at 20,800 g for 10 minutes. All stock solutions of imatinib and N-DMI were prepared in methanol. All incubations (including controls) contained the same concentration of organic solvent (1% methanol or 0.5%:0.5% methanol:acetonitrile). As appropriate, the incubation time was optimized within the linear range for metabolite formation depending on the turnover conditions of each specific experiment. The unbound fraction of 0.1 µM imatinib in microsomal incubations had previously been determined (Filppula et al., 2012), and the nonspecific binding of N-DMI to microsomes was assumed to equal that of imatinib.

Measurement of imatinib and its metabolites.

Imatinib and N-DMI concentrations were quantified by use of an API 3000 liquid chromatography-tandem mass spectrometry system (Sciex Division of MDS Inc, Toronto, ON, Canada). Concentrations of imatinib and N-DMI were measured in positive turbo ion spray mode. Chromatography was performed on an Atlantis Hilic Silica analytic column (2.1×100 mm, 3.0 µm) (Waters, Milford, MA, USA) by use of gradient elution. The mobile phase was (A) 10 mM ammonium formate in 0.1% HCOOH, and (B) 0.1% HCOOH in acetonitrile:MeOH 10:1, v/v, and the gradient comprised 0 min at 95% (B), 15 min to 50% (B), 5 min at 50% (B), 0.1 min to 95% (B), and finally 14.9 min at 95% (B). The flow rate was 0.2 ml/min. The mass spectrometer was operated in multi reaction mode (MRM) and ion transitions monitored were m/z (mass-to-charge ratio) 494.3 to 394.3 for imatinib, 480.3 to 394.3 for N-DMI, 502.2 to 394.3 for imatinib-d8 and 488.2 to 394.3 for N-DMI-d8. The peaks of a hydroxy benzylic metabolite (M5), piperidine N-oxide imatinib (M6) and pyridine N-oxide imatinib (M8) were monitored during the assays based on ion transitions reported (Marull and Rochat, 2006; Rochat et al., 2008), and their quantities were measured as arbitrary units relative to the ratio of the peak height of the metabolite to the peak height of N-DMI-d8. The limit of quantification was 0.005 µM for imatinib, 0.01 µM for N-DMI, and a signal/noise ratio of 10:1 was used as the limit of quantification for

DMD Fast Forward. Published on October 1, 2012 as DOI: 10.1124/dmd.112.048017
This article has not been copyedited and formatted. The final version may differ from this version.

M5, M6, and M8. For imatinib and N-DMI, the between-day coefficient of variation (CV) was <15% at relevant concentrations.

Recombinant P450 isoform studies.

First, the depletion of 0.1 µM imatinib by CYP1A2 (50 pmol/ml), CYP2A6 (30 pmol/ml), CYP2B6 (40 pmol/ml), CYP2C8 (158 pmol/ml), CYP2C9 (120 pmol/ml), CYP2C19 (174 pmol/ml), CYP2D6 (72 pmol/ml), CYP2E1 (296 pmol/ml), CYP3A4 (66 pmol/ml), and CYP3A5 (50 pmol/ml) was investigated in a 30 min incubation. Then, metabolite formation by these enzymes was studied by incubating 1 µM imatinib with each enzyme for up to 60 min. Finally, the enzyme kinetics of N-DMI formation was determined by incubating imatinib (0.10-320 µM) with CYP2C8 (33 pmol/ml) for 4 min, CYP3A4 (13 pmol/ml) for 3 min, and CYP3A5 (10 pmol/ml) for 30 min. The protein concentration was 0.5 mg/ml in the depletion and metabolite formation studies, and 0.1 mg/ml in the enzyme kinetic incubations.

Effects of CYP-selective inhibitors on imatinib metabolism.

In order to confirm the results from the recombinant P450 studies, inhibition studies with HLM were carried out. Montelukast (5 µM), sulfaphenazole (10 µM), omeprazole (10 µM), quinidine (10 µM), and ketoconazole (1 µM) were tested as competitive inhibitors of CYP2C8, CYP2C9, CYP2C19, CYP2D6, and CYP3A4, respectively (Baldwin et al., 1995; Newton et al., 1995; Bourrie et al., 1996; Ko et al., 1997; Eagling et al., 1998; Walsky et al., 2005). Furafylline (20 µM), 8-M-P (0.5 µM), clopidogrel (1 µM), GEM-G (60 µM), DDC (100 µM), and troleandomycin (50 µM) were examined as mechanism-based inhibitors of CYP1A2, CYP2A6, CYP2B6, CYP2C8, CYP2E1, and CYP3A4, respectively (Newton et al., 1995; Bourrie et al., 1996; Draper et al., 1997; Koenigs et al., 1997; Eagling et al., 1998; Richter et al., 2004; Ogilvie et al., 2006). 1 µM imatinib was incubated with each inhibitor (or after preincubation), and metabolite formation rate was measured. Then, selected inhibitors (GEM-G, montelukast, ketoconazole, and troleandomycin) were incubated with 0.1 µM imatinib for up to 60 min.

Metabolism of N-DMI.

The further metabolism of N-DMI was investigated by incubating 0.1 and 1 µM N-DMI with 0.5 mg/ml HLM and following its depletion for up to 60 min. N-DMI (0.1 µM) was also incubated for 30 min with CYP1A2 (50 pmol/ml), CYP2C8 (158 pmol/ml), CYP2D6 (72 pmol/ml), CYP3A4 (66 pmol/ml), CYP3A5 (50 pmol/ml), and an enzyme mix containing CYP2A6 (59 pmol/ml), CYP2B6 (7.7 pmol/ml),

CYP2C9 (24 pmol/ml), CYP2C19 (35 pmol/ml), and CYP2E1 (25 pmol/ml), wherein the total protein concentration was 0.5 mg/ml. Finally, the depletion of 0.05 µM N-DMI by CYP2C8, CYP3A4, and CYP3A5 was examined in detail.

Data analysis.

The kinetics of N-DMI formation were analyzed using SigmaPlot software (version 9.01; Systat Software, Inc., San Jose, CA). Selection of the best-fit enzyme model was based on the Akaike information criterion, on R^2, and on the examination of Michaelis-Menten plots. For CYP2C8 and CYP3A4, the results were best described by an uncompetitive substrate inhibition model: $v = V_{max} \times S / (K_m \times S \times S^2 / K_i)$, where v is velocity (pmol/min/pmol), V_{max} is the maximal velocity (pmol/min/pmol), S is substrate concentration (µM), K_m is the Michaelis-Menten constant (µM), and K_i is the inhibitory constant (µM). CYP3A5-mediated N-demethylation was best described by traditional Michael-Menten kinetics: $v = V_{max} \times S / (K_m \times S)$. Intrinsic clearance for N-DMI formation ($CL_{int, N\text{-}DMI\ form}$) was calculated according to $CL_{int, N\text{-}DMI\ form} = V_{max} / K_m$. Pseudo-first-order depletion rate constants (k_{dep}) were determined for the depletion of 0.1 µM imatinib, and 0.05 and 0.1 µM N-DMI in HLM and recombinant enzyme incubations using nonlinear regression analysis (SigmaPlot). Imatinib k_{dep} values were calculated on the basis of the time points at 0-8 min for CYP2C8, 0-4 min for CYP3A4, 0-30 min for the other P450 isoforms and HLM. N-DMI k_{dep} values were estimated based on time points at 0-30 min for all P450 isoforms and 0-60 min for HLM. Percent inhibition of imatinib depletion was calculated by comparing k_{dep} values to those of control incubations. Assuming that imatinib and N-DMI concentrations were $<<K_m$ for their metabolic pathways, their intrinsic clearance in depletion experiments was expressed as $CL_{int, dep} = k_{dep} / [M]$, where [M] is the microsomal protein concentration or P450 concentration in recombinant enzyme incubations (Venkatakrishnan et al., 2003). In addition, an intrinsic clearance value for the formation of all primary metabolites of imatinib other than N-DMI was defined as $CL_{int,u, ima\ dep} - CL_{int,u, N\text{-}DMI\ form}$ for each P450 isoform, where $CL_{int,u, ima\ dep}$ and $CL_{int,u, N\text{-}DMI\ form}$ denote the unbound intrinsic clearance values for imatinib depletion and N-DMI formation, respectively. To estimate the relative contributions of different P450 enzymes to imatinib and N-DMI metabolism, the CL_{int} values, adjusted for nonspecific binding in microsomes, were multiplied with intersystem extrapolation factors (ISEFs)(Proctor et al., 2004) of each P450 isoform and with average P450 isoform abundance (pmol/mg microsomal protein)(Table 1). The obtained values were then scaled to *in vivo* using 40 mg of microsomal protein per gram liver (Houston and Galetin, 2008) and

DMD Fast Forward. Published on October 1, 2012 as DOI: 10.1124/dmd.112.048017
This article has not been copyedited and formatted. The final version may differ from this version.

25.7 g of liver weight per kg body weight (Davies and Morris, 1993). Hepatic blood clearance (CL_H) values were calculated using the well-stirred model: $CL_H = Q_h \times f_{u,b} \times CL_{int,\ in\ vivo} / [Q_h + (f_{u,b} \times CL_{int,\ in\ vivo})]$ where Q_h is the hepatic blood flow (20.7 ml/min/kg)(Houston and Galetin, 2008), $f_{u,b}$ is the unbound fraction of imatinib or N-DMI in blood, and $CL_{int,\ in\ vivo}$ is the scaled CL_{int}.

***In silico* study**

Construction and validation of a Simcyp model for imatinib.

Based on the present *in vitro* investigations and literature data, compound files for imatinib and N-DMI (see Supplementary Tables S1 and S2 for data) were constructed within the Simcyp Population-Based Simulator (V11.00; Simcyp Limited, UK). Using physiologically-based pharmacokinetic (PBPK) modeling, Simcyp simulates change in drug concentration over time. The software generates virtual populations reflecting variability in genetic, physiological, and demographic variables using Monte Carlo methods so that interindividual variability in drug elimination and the importance of different metabolizing P450 isoforms in a population can be assessed (Howgate et al., 2006; Rostami-Hodjegan and Tucker, 2007; Jamei et al., 2009; Rowland Yeo et al., 2010).

The models for imatinib and N-DMI comprised first order oral absorption from the intestine (for imatinib), intestinal metabolism, a minimal physiologically-based distribution model including a single adjusting compartment, and elimination by hepatic CYP-mediated and additional (non CYP-mediated) metabolism and by renal excretion. The hepatic elimination input parameters were obtained from the present *in vitro* studies. ISEF factors in Tables 1 and 2 and other parameters provided by the software were used to scale CL_{int} to CL_H, and CL_H values were then predicted using the well-stirred model. Renal clearance was estimated from literature values of systemic clearance and amount excreted unchanged in the urine (Bornhauser et al., 2005; Gschwind et al., 2005). Then, hepatic and renal clearances were combined with additional clearance to derive the total clearance. Furthermore, the compound files for imatinib and N-DMI included values for direct inhibition of different P450 enzymes, and the final model for imatinib also included kinetic constants for MBI of CYP3A4. When the literature and experimental values had been entered into the compound files, the model was refined by adjusting the additional clearance and the volume of the single adjusting compartment so that published single dose pharmacokinetic data could be described accurately (see Supplementary Methods and Supplementary Table S3 for details). Thereafter, the model was validated by comparing

simulations to published multiple-dose pharmacokinetic studies, and to interaction studies with ketoconazole, ritonavir, and rifampicin (Supplementary Methods and Supplementary Tables S4-S5).

Simulation of the clinical consequences of* in vitro *findings.

To demonstrate the significance of MBI of CYP3A4 to the metabolism of imatinib, multiple-dose pharmacokinetics of imatinib 400 mg once daily were simulated, both with and without MBI. In addition, the time- and dose-dependent effects of imatinib on intestinal and hepatic CYP3A4 activity, and on the roles of CYP2C8 and CYP3A4 in imatinib biotransformation were simulated using the final model and imatinib doses ranging from 100 mg once daily to 400 mg twice daily (Supplementary Methods and Supplementary Table S4). Furthermore, the effects of CYP2C8 polymorphisms and of a strong CYP2C8 inhibitor (gemfibrozil 600 mg twice daily), strong CYP3A4 inhibitor (itraconazole 100 mg twice daily) or their combination on imatinib pharmacokinetics after a single dose and/or multiple doses of imatinib 400 mg once daily were predicted as detailed in the Supplementary Methods and Supplementary Tables S6-S8.

Results

In vitro study

Imatinib metabolism by recombinant enzymes.

Recombinant CYP2C8 and CYP3A4 metabolized 0.1 and 1 μM imatinib rapidly and <13% of the parent drug remained after 30 min incubation (Fig. 1A and 2A). In CYP3A5 incubations ~80% of imatinib was left at 30 min, whereas the other P450 isoforms tested had a minor effect on imatinib concentrations (>90% of parent drug was left). At 1 μM imatinib, N-demethylation was mediated by CYP2C8, CYP3A4, and CYP3A5, but very small amounts of N-DMI were formed also by CYP2D6, CYP2C19 and CYP2C9 (Fig. 1B). However, at 0.1 μM imatinib, only CYP2C8, CYP3A4 and CYP3A5 formed detectable amounts of N-DMI (Fig. 1B and 2B). At 1 μM imatinib, CYP2C8 also formed detectable amounts of M6, and CYP2D6 catalyzed formation of M5, whereas CYP3A4 formed both M5 and M6 (data not shown). The enzyme kinetics of N-DMI formation by CYP2C8, CYP3A4, and CYP3A5 is presented in Fig. 2C.

Comparison of CL_{int} values obtained from the depletion (total metabolism) of 0.1 μM imatinib and N-demethylation kinetics, indicated that formation of N-DMI accounts for the majority (88%) of imatinib metabolism by CYP2C8, whereas the metabolite accounts for 27% and 75% of imatinib metabolism by CYP3A4 and CYP3A5 (Table 1), respectively. With use of the static ISEF approach, CYP2C8 and CYP3A4 were estimated to be the most important enzymes in imatinib metabolism *in vivo* (contributions of 40% and 57%, respectively, with <3% contribution by other P450 isoforms; Table 1).

Effects of CYP-selective inhibitors on imatinib metabolism.

The CYP2C8 inhibitors montelukast and GEM-G, and the CYP3A4 inhibitors ketoconazole and troleandomycin inhibited the formation of N-DMI by ≥50% (Fig. 1C) and were further investigated in a depletion study. Herein, montelukast and GEM-G inhibited the depletion of 0.1 μM imatinib by ~45%, whereas the CYP3A4 inhibitors inhibited it by almost 80% (data not shown).

Metabolism of N-DMI.

The further metabolism of N-DMI was mainly catalyzed by CYP3A4, with a less significant contribution by CYP2C8, and minor contribution by other P450 enzymes (Fig. 1D and 2D). Incubation with a

DMD Fast Forward. Published on October 1, 2012 as DOI: 10.1124/dmd.112.048017
This article has not been copyedited and formatted. The final version may differ from this version.

mixture containing CYP2A6, CYP2B6, CYP2C9, CYP2C19, and CYP2E1 did not lead to significant depletion of N-DMI. Using the ISEF approach, the contribution of CYP3A4 to the hepatic metabolism of N-DMI *in vivo* was estimated to average 40%, followed by CYP2C8 (11%), whereas the contributions by CYP1A2, CYP2D6 and CYP3A5 were <5% each (Table 2).

***In silico* study**

Comparison of a PBPK model of imatinib to its clinical pharmacokinetics.

Based on physical-chemical and pharmacokinetic data available from the literature, a PBPK model was created to estimate the contributions of different P450 enzymes to imatinib and N-DMI metabolism in humans over time. The clearances of imatinib and N-DMI were predicted on the basis of the present *in vitro* data together with literature data on renal and additional clearance, and the final model included MBI of CYP3A4 by imatinib. The simulated concentration-time curves as well as the mean pharmacokinetic parameters of imatinib and N-DMI matched well with published data on imatinib single dose pharmacokinetics in healthy volunteers (Fig. 3A-B, Supplementary Table S3).

Compared to when only direct inhibition of CYP3A4 by imatinib was considered, the final model simulated the peak concentrations, $AUC_{0\text{-}24}$, and trough concentrations of imatinib on day 30 that were on average 32%, 58%, and 113% higher, respectively, and those of N-DMI were on average 5%, 16%, and 24% higher, respectively (Fig. 4A-B). The final model also matched well with observed trough and peak concentrations of imatinib during treatment with 400 mg once daily, averaging 910-1,530 ng/ml and 2,200-3,405 ng/ml, respectively, and with those of N-DMI averaging 170-301 ng/ml and 290-556 ng/ml, respectively (Peng et al., 2004b; van Erp et al., 2007; Gibbons et al., 2008; Demetri et al., 2009; Kim et al., 2011; Teng et al., 2012) (Fig. 4A-B, Supplementary Table S4). Similarly, the simulations predicted well the effects of ketoconazole, rifampicin and ritonavir on the pharmacokinetics of imatinib (Supplementary Table S5). The validation simulation of gemfibrozil pharmacokinetics is presented in Supplementary Fig. S2.

Role of CYP2C8 in imatinib metabolism is important during prolonged treatment.

With the final model, the inactivation of intestinal and hepatic CYP3A4 by imatinib proceeded time- and dose-dependently (Fig. 4A-E). For example, at steady-state, imatinib 100 mg once daily, 400 mg once daily, and 400 mg twice daily, was predicted to reduce the amount of active CYP3A4 to 55%-

59%, 22%-29%, and 13%-15% of its normal amount in the liver, respectively. At the commencement of imatinib treatment, the fractions metabolized by hepatic CYP3A4 and CYP2C8 were predicted to average 59% and 39% of the total hepatic clearance of imatinib, equaling those estimated with the static ISEF model. After multiple doses of imatinib 400 mg once daily, the majority of the hepatic metabolism of imatinib was predicted to occur by CYP2C8 (61%-65%) and a smaller proportion by CYP3A4 (31%-37%)(Fig. 4E). The corresponding values for treatment with 400 mg twice daily were 71%-74% and 22%-25% for CYP2C8 and CYP3A4, respectively.

An otherwise typical 60-year old male, but with a two-fold higher than the average CYP2C8 activity in the liver, was predicted to have a markedly increased steady-state imatinib metabolism (Fig. 5A-B). His plasma concentrations of imatinib were for the most part of the 24 h-dosing interval below the suggested effectiveness threshold of about 1,000 ng/ml (Fig. 5A). Conversely, a low activity CYP2C8 genotype (50% reduction in CYP2C8 activity) decreased imatinib metabolism, leading to increased imatinib concentrations and reduced N-DMI concentrations.

According to drug-drug interaction predictions, a strong CYP3A4 inhibitor (itraconazole) increased the $AUC_{0-\infty}$ of imatinib and N-DMI by 38% and 6%, respectively, after a single dose of imatinib 400 mg (Fig. 5C-D, Supplementary Table S8), and the dosing interval AUC by 18% and 6%, respectively, following multiple imatinib doses (Fig. 5E-F). A strong CYP2C8 inhibitor (gemfibrozil) was predicted to increase the $AUC_{0-\infty}$ of a single dose of imatinib 1.8-fold, and the dosing interval AUC after multiple imatinib doses 2.3-fold, whereas it reduced the AUC of N-DMI by 59%-84%. The inhibition of both CYP2C8 and CYP3A4 was predicted to markedly increase imatinib AUC 2.9-fold, and almost completely inhibit N-DMI formation (by >79%).

DMD Fast Forward. Published on October 1, 2012 as DOI: 10.1124/dmd.112.048017
This article has not been copyedited and formatted. The final version may differ from this version.

Discussion

According to the present *in vitro* findings, imatinib metabolism is almost exclusively mediated by CYP2C8 and CYP3A4 at clinically relevant imatinib concentrations. Formation of the active metabolite of imatinib, N-DMI, accounted for the majority of imatinib metabolism by CYP2C8, whereas more than two thirds of imatinib metabolism mediated by CYP3A4 occurred via other metabolic pathways. Moreover, the further biotransformation of N-DMI was mainly catalyzed by CYP3A4. Pharmacokinetic simulations based on these results and on recent data indicating that imatinib is an irreversible mechanism-based inhibitor of CYP3A4 (Filppula et al., 2012), predicted that the role of CYP3A4 in imatinib metabolism is important mainly in the beginning of therapy, but diminishes thereafter, because of time-dependent autoinhibition of CYP3A4-mediated metabolism of imatinib. Consequently, CYP2C8 is likely to be the most important enzyme in imatinib metabolism at steady-state, during long-term treatment.

Imatinib biotransformation occurs via multiple metabolic pathways in addition to the N-demethylation pathway (Gschwind et al., 2005; Marull and Rochat, 2006; Rochat et al., 2008). Therefore, we used a depletion approach to estimate the contributions of different P450 enzymes to the total elimination of imatinib at low, therapeutic concentrations. The depletion rates and inhibition experiments showed that CYP2C8 and CYP3A4 almost exclusively mediate the hepatic microsomal metabolism of imatinib with other isoforms contributing to a minor extent (~5%). For example, CYP3A5 metabolized imatinib to N-DMI, but the total elimination CL_{int} of CYP3A5 was small (<10% of that of CYP2C8). Comparison of CL_{int} values obtained from the depletion of 0.1 µM imatinib and N-demethylation kinetics indicated that N-demethylation accounts for the majority of imatinib metabolism by CYP2C8. On the contrary, CYP3A4 seemed to produce more than twice as much other metabolites as its produced N-DMI, in line with previous data (Rochat et al., 2008). In our incubations, CYP3A4 formed M5 and M6, but due to lack of authentic standards, the quantitative evaluation of these metabolites was not possible. CYP2D6 also formed a small amount of M5, but the depletion experiment with 0.1 µM imatinib indicated a negligible significance for CYP2D6 in its metabolism. Also CYP2C9, CYP2C19, CYP1A1, CYP1B1, and CYP4F may play minor roles in imatinib biotransformation (http://www.accessdata.fda.gov/drugsatfda_docs/nda/2001/21335_Gleevec.cfm) (Rochat et al., 2008), but in our study the contributions of CYP2C9 and CYP2C19 were negligible at therapeutic concentrations, and CYP1A1, CYP1B1, and CYP4F were not investigated because of their

insignificant hepatic expression. Moreover, our findings indicate that the further metabolism of N-DMI is mediated mainly by CYP3A4, with CYP2C8, CYP3A5, CYP2D6, and CYP1A2 participating to a smaller extent.

Using the static ISEF approach, the contributions of CYP2C8 and CYP3A4 to the hepatic metabolism of imatinib *in vivo* were estimated to be 40% and 57%, respectively. However, because imatinib inactivates CYP3A4 time-dependently (Filppula et al., 2012), a static model cannot adequately describe the contributions of different P450 enzymes to imatinib metabolism. Therefore, we constructed a dynamic PBPK model for imatinib and N-DMI pharmacokinetics, incorporating previous data on time-dependent inactivation of CYP3A4 by imatinib. Interaction simulations with ketoconazole, rifampicin, and ritonavir, based on this model, generally showed a good agreement with their reference studies (Bolton et al., 2004; Dutreix et al., 2004; van Erp et al., 2007). Thus, it seems that our *in vitro* data for CYP3A4 generated reliable predictions of its role in imatinib pharmacokinetics. Compared to a model without MBI of CYP3A4 by imatinib, steady-state simulations based on the final model corresponded much better with clinical data showing that trough and peak concentrations average 910-1,530 ng/ml and 2,200-3,405 ng/ml, respectively, during imatinib 400 mg once daily (Peng et al., 2004b; van Erp et al., 2007; Gibbons et al., 2008; Demetri et al., 2009; Kim et al., 2011; Teng et al., 2012).

MBI of P450 enzymes proceeds in a time- and concentration-dependent manner, because it requires that the inhibitor is metabolized by the enzyme to an intermediate, which immediately binds covalently to the enzyme (Lin and Lu, 1998). Thus, unlike reversible inhibitors, mechanism-based inhibitors inactivate their victim enzymes permanently, and enzyme activity can be regained only by synthesis of new enzyme. Clinically, these characteristics can lead to a slow onset of inhibition and a long-lasting duration of inhibition. MBI poses a particular problem when *in vitro* studies are carried out to estimate the contributions of P450 enzymes to the metabolism of a drug, which is a mechanism-based inhibitor of a P450 form participating in its own metabolism. Failure to consider MBI leads to overestimation of the role of this enzyme. To overcome this problem with imatinib, we used very short incubations and low imatinib concentrations in order to minimize MBI and obtain reliable initial rates of *in vitro* metabolism, and applied a dynamic PBPK model for extrapolation of our *in vitro* data to *in vivo*.

DMD Fast Forward. Published on October 1, 2012 as DOI: 10.1124/dmd.112.048017
This article has not been copyedited and formatted. The final version may differ from this version.

According to our simulations, autoinhibition of the CYP3A4-mediated metabolism of imatinib is likely to attribute a key role for CYP2C8 in imatinib elimination. The fraction of hepatic clearance mediated by CYP2C8 was simulated to increase from 40% in the beginning of treatment to over 60% after multiple doses of imatinib 400 mg once daily. Conversely, the fraction eliminated by CYP3A4 decreased from 60% in the beginning to <40% during multiple dosing. The significance of CYP2C8 in steady-state imatinib pharmacokinetics became apparent in interaction simulations, where a strong CYP2C8 inhibitor like gemfibrozil (Backman et al., 2002; Honkalammi et al., 2012) was predicted to increase imatinib AUC, following a single imatinib dose, by 80%, and after multiple imatinib doses by 130%. By contrast, a strong CYP3A4 inhibitor like itraconazole (Olkkola et al., 1994) was predicted to increase imatinib AUC by 40% after a single dose of imatinib, and by 20% only, after multiple imatinib doses. This result is comparable to clinical findings from interaction studies with ketoconazole and ritonavir (Dutreix et al., 2004; van Erp et al., 2007). According to our simulations, gemfibrozil could reduce the plasma exposure to N-DMI by up to 85%, whereas itraconazole could increase it by ~5%. Of note, the combination of gemfibrozil and itraconazole was predicted to increase imatinib $AUC_{0-\tau}$ by almost 200% during multiple dosing, highlighting the potential dangers of multiple interacting medications.

Simcyp has been associated with overpredictions of the magnitude of time-dependent drug-drug interactions. For CYP3A4, the former default degradation rate constant of 0.0077 1/h has been recognized as an important source for overpredictions, whereas the value of 0.019 1/h, used in version 11, has generated relatively reliable predictions (Rowland Yeo et al., 2011). Other possible factors impairing prediction accuracy of drug-drug interactions are failure to consider transporter mechanisms, gut metabolism or simultaneous mechanisms such as concurrent inhibition and induction of enzymes (Peters et al., 2012). In the present work, as evident from steady state simulations and interaction simulations with the CYP3A4 inhibitors, Simcyp did not appear to overpredict the impact of autoinhibition of CYP3A4 on imatinib pharmacokinetics. However, the effect of imatinib on the pharmacokinetics of other CYP3A4 substrates was not investigated in this work and needs to be addressed in future studies. Furthermore, given the above uncertainties, clinical studies are needed to evaluate the prediction accuracy concerning the role of CYP2C8 in imatinib pharmacokinetics and interactions.

There is a wide interindividual variability in imatinib plasma concentrations, associated with nonresponse and disease progression, even in the absence of interacting comedications (Peng et al.,

2004b; Picard et al., 2007; Teng et al., 2012). Differences in CYP3A4 activity have been suggested to partly explain this variability (Peng et al., 2005; Apperley, 2007). Our findings contrast this suggestion and raise the possibility that pharmacogenetic polymorphisms of CYP2C8 can affect imatinib plasma concentrations, especially during long-term medication. For example, the *CYP2C8*3* allele has been associated with a considerably increased clearance of several drugs, such as rosiglitazone and pioglitazone (Kirchheiner et al., 2006; Tornio et al., 2008; Aquilante et al., 2012). In our simulations, a high activity CYP2C8 genotype was predicted to result in an increased imatinib metabolism, leading to mean plasma levels of imatinib below the threshold concentration of 1,000 ng/ml, suggesting that genetic polymorphisms of CYP2C8 could possibly affect the pharmacokinetics of imatinib to a clinically relevant degree. It should be noted, however, that the effect of the *CYP2C8*3* polymorphism seems to be substrate-dependent and therefore clinical studies with imatinib are needed. Moreover, imatinib is a substrate and inhibitor of several transporters *in vitro*, but their clinical significance in imatinib pharmacokinetics has not yet been established, apart from the role of organic cation transporter 1 (OCT1) in uptake of imatinib to leukocytes and leukemic cells (Eechoute et al., 2011; Wang et al., 2012). Our interaction simulations (Fig 5C-F) did not account for possible co-effects of P450 inhibitors on different transporter functions, which could influence imatinib pharmacokinetics. Thus, an inhibition or induction of relevant transporters affecting imatinib pharmacokinetics could modify the effect of CYP2C8 and CYP3A4 inhibitors on imatinib plasma and tissue concentrations.

In this work, we used an integrated approach of carefully optimized *in vitro* experiments, comprising both depletion and enzyme kinetic experiments, and pharmacokinetic simulations to evaluate the clinical relevance of CYP2C8 and CYP3A4 in imatinib elimination. Although clinical studies are necessary to confirm our *in vitro-in silico* findings, it is likely that imatinib time-dependently inhibits its own CYP3A4-mediated metabolism, leading to a key role for CYP2C8 in its elimination. Thus, during multiple dosing, both pharmacogenetic polymorphisms and drug interactions affecting CYP2C8 activity may cause marked interindividual variability in the exposure and response to imatinib. Overall, the present findings highlight the need to carefully evaluate the implications of MBI using integrated *in vitro* and modeling/simulation approaches.

Authorship Contributions

Participated in research design: Filppula, Neuvonen M., Laitila, Neuvonen P.J., and Backman

Conducted experiments: Filppula, Neuvonen M., Laitila, and Backman

Performed data analysis: Filppula, Neuvonen P.J., and Backman

Wrote or contributed to the writing of the manuscript: Filppula, Neuvonen M., Laitila, Neuvonen P.J., and Backman

References

Apperley JF (2007) Part I: Mechanisms of resistance to imatinib in chronic myeloid leukaemia. *Lancet Oncology* **8:**1018-1029.

Aquilante CL, Kosmiski LA, Bourne DW, Bushman L, Daily EB, Hammond KP, Hopley CW, Kadam RS, Kanack AT, Kompella UB, Le M, Predhomme JA, Rower JE, and Sidhom MS (2012) Impact of the CYP2C8*3 polymorphism on the drug-drug interaction between gemfibrozil and pioglitazone. *Br J Clin Pharmacol* doi: 10.1111/j.1365-2125.2012.04343.x.

Backman JT, Kyrklund C, Neuvonen M, and Neuvonen PJ (2002) Gemfibrozil greatly increases plasma concentrations of cerivastatin. *Clin Pharmacol Ther* **72:**685-691.

Baldwin SJ, Bloomer JC, Smith GJ, Ayrton AD, Clarke SE, and Chenery RJ (1995) Ketoconazole and sulphaphenazole as the respective selective inhibitors of P4503A and 2C9. *Xenobiotica* **25:**261-270.

Bolton AE, Peng B, Hubert M, Krebs-Brown A, Capdeville R, Keller U, and Seiberling M (2004) Effect of rifampicin on the pharmacokinetics of imatinib mesylate (Gleevec, STI571) in healthy subjects. *Cancer Chemother Pharmacol* **53:**102-106.

Bornhauser M, Pursche S, Bonin M, Freiberg-Richter J, Jenke A, Illmer T, Ehninger G, and Schleyer E (2005) Elimination of imatinib mesylate and its metabolite N-desmethyl-imatinib. *J Clin Oncol* **23:**3855-3856.

Bourrie M, Meunier V, Berger Y, and Fabre G (1996) Cytochrome P450 isoform inhibitors as a tool for the investigation of metabolic reactions catalyzed by human liver microsomes. *J Pharmacol Exp Ther* **277:**321-332.

Davies B and Morris T (1993) Physiological parameters in laboratory animals and humans. *Pharm Res* **10:**1093-1095.

Demetri GD, Wang Y, Wehrle E, Racine A, Nikolova Z, Blanke CD, Joensuu H, and von Mehren M (2009) Imatinib plasma levels are correlated with clinical benefit in patients with unresectable/metastatic gastrointestinal stromal tumors. *J Clin Oncol* **27:**3141-3147.

Draper AJ, Madan A, and Parkinson A (1997) Inhibition of coumarin 7-hydroxylase activity in human liver microsomes. *Arch Biochem Biophys* **341:**47-61.

Duffaud F and Le Cesne A (2009) Imatinib in the treatment of solid tumours. *Target Oncol* **4:**45-56.

Dutreix C, Peng B, Mehring G, Hayes M, Capdeville R, Pokorny R, and Seiberling M (2004) Pharmacokinetic interaction between ketoconazole and imatinib mesylate (Glivec) in healthy subjects. *Cancer Chemother Pharmacol* **54:**290-294.

Eagling VA, Tjia JF, and Back DJ (1998) Differential selectivity of cytochrome P450 inhibitors against probe substrates in human and rat liver microsomes. *Br J Clin Pharmacol* **45:**107-114.

Eechoute K, Sparreboom A, Burger H, Franke RM, Schiavon G, Verweij J, Loos WJ, Wiemer EA, and Mathijssen RH (2011) Drug transporters and imatinib treatment: implications for clinical practice. *Clin Cancer Res* **17:**406-415.

Filppula AM, Laitila J, Neuvonen PJ, and Backman JT (2012) Potent mechanism-based inhibition of CYP3A4 by imatinib explains its liability to interact with CYP3A4 substrates. *Br J Pharmacol* **165:**2787-2798.

Gibbons J, Egorin MJ, Ramanathan RK, Fu P, Mulkerin DL, Shibata S, Takimoto CH, Mani S, LoRusso PA, Grem JL, Pavlick A, Lenz HJ, Flick SM, Reynolds S, Lagattuta TF, Parise RA, Wang Y, Murgo AJ, Ivy SP, and Remick SC (2008) Phase I and pharmacokinetic study of

imatinib mesylate in patients with advanced malignancies and varying degrees of renal dysfunction: a study by the National Cancer Institute Organ Dysfunction Working Group. *J Clin Oncol* **26:**570-576.

Gschwind HP, Pfaar U, Waldmeier F, Zollinger M, Sayer C, Zbinden P, Hayes M, Pokorny R, Seiberling M, Ben-Am M, Peng B, and Gross G (2005) Metabolism and disposition of imatinib mesylate in healthy volunteers. *Drug Metab Dispos* **33:**1503-1512.

Honkalammi J, Niemi M, Neuvonen PJ, and Backman JT (2012) Gemfibrozil is a strong inactivator of CYP2C8 in very small multiple doses. *Clin Pharmacol Ther* **91:**846-855.

Houston JB and Galetin A (2008) Methods for predicting in vivo pharmacokinetics using data from in vitro assays. *Curr Drug Metab* **9:**940-951.

Howgate EM, Rowland Yeo K, Proctor NJ, Tucker GT, and Rostami-Hodjegan A (2006) Prediction of in vivo drug clearance from in vitro data. I: impact of inter-individual variability. *Xenobiotica* **36:**473-497.

Jamei M, Dickinson GL, and Rostami-Hodjegan A (2009) A framework for assessing inter-individual variability in pharmacokinetics using virtual human populations and integrating general knowledge of physical chemistry, biology, anatomy, physiology and genetics: A tale of 'bottom-up' vs 'top-down' recognition of covariates. *Drug Metab Pharmacokinet* **24:**53-75.

Kim DW, Tan EY, Jin Y, Park S, Hayes M, Demirhan E, Schran H, and Wang Y (2011) Effects of imatinib mesylate on the pharmacokinetics of paracetamol (acetaminophen) in Korean patients with chronic myelogenous leukaemia. *Br J Clin Pharmacol* **71:**199-206.

Kirchheiner J, Thomas S, Bauer S, Tomalik-Scharte D, Hering U, Doroshyenko O, Jetter A, Stehle S, Tsahuridu M, Meineke I, Brockmoller J, and Fuhr U (2006) Pharmacokinetics and

pharmacodynamics of rosiglitazone in relation to CYP2C8 genotype. *Clin Pharmacol Ther* **80:**657-667.

Ko JW, Sukhova N, Thacker D, Chen P, and Flockhart DA (1997) Evaluation of omeprazole and lansoprazole as inhibitors of cytochrome P450 isoforms. *Drug Metab Dispos* **25:**853-862.

Koenigs LL, Peter RM, Thompson SJ, Rettie AE, and Trager WF (1997) Mechanism-based inactivation of human liver cytochrome P450 2A6 by 8-methoxypsoralen. *Drug Metab Dispos* **25:**1407-1415.

Kovacsovics T and Maziarz RT (2006) Philadelphia chromosome-positive acute lymphoblastic leukemia: impact of imatinib treatment on remission induction and allogeneic stem cell transplantation. *Curr Oncol Rep* **8:**343-351.

Larson RA, Druker BJ, Guilhot F, O'Brien SG, Riviere GJ, Krahnke T, Gathmann I, and Wang Y (2008) Imatinib pharmacokinetics and its correlation with response and safety in chronic-phase chronic myeloid leukemia: a subanalysis of the IRIS study. *Blood* **111:**4022-4028.

Lin JH and Lu AY (1998) Inhibition and induction of cytochrome P450 and the clinical implications. *Clin Pharmacokinet* **35:**361-390.

Marull M and Rochat B (2006) Fragmentation study of imatinib and characterization of new imatinib metabolites by liquid chromatography-triple-quadrupole and linear ion trap mass spectrometers. *J Mass Spectrom* **41:**390-404.

Nebot N, Crettol S, d'Esposito F, Tattam B, Hibbs DE, and Murray M (2010) Participation of CYP2C8 and CYP3A4 in the N-demethylation of imatinib in human hepatic microsomes. *Br J Pharmacol* **161:**1059-1069.

Newton DJ, Wang RW, and Lu AY (1995) Cytochrome P450 inhibitors. Evaluation of specificities in the in vitrometabolism of therapeutic agents by human liver microsomes. *Drug Metab Dispos* **23:**154-158.

Nikolova Z, Peng B, Hubert M, Sieberling M, Keller U, Ho YY, Schran H, and Capdeville R (2004) Bioequivalence, safety, and tolerability of imatinib tablets compared with capsules. *Cancer Chemother Pharmacol* **53:**433-438.

Ogilvie BW, Zhang D, Li W, Rodrigues AD, Gipson AE, Holsapple J, Toren P, and Parkinson A (2006) Glucuronidation converts gemfibrozil to a potent, metabolism-dependent inhibitor of CYP2C8: implications for drug-drug interactions. *Drug Metab Dispos* **34:**191-197.

Olkkola KT, Backman JT, and Neuvonen PJ (1994) Midazolam should be avoided in patients receiving the systemic antimycotics ketoconazole or itraconazole. *Clin Pharmacol Ther* **55:**481-485.

Peng B, Dutreix C, Mehring G, Hayes MJ, Ben-Am M, Seiberling M, Pokorny R, Capdeville R, and Lloyd P (2004a) Absolute bioavailability of imatinib (Glivec) orally versus intravenous infusion. *J Clin Pharmacol* **44:**158-162.

Peng B, Hayes M, Resta D, Racine-Poon A, Druker BJ, Talpaz M, Sawyers CL, Rosamilia M, Ford J, Lloyd P, and Capdeville R (2004b) Pharmacokinetics and pharmacodynamics of imatinib in a phase I trial with chronic myeloid leukemia patients. *J Clin Oncol* **22:**935-942.

Peng B, Lloyd P, and Schran H (2005) Clinical pharmacokinetics of imatinib. *Clin Pharmacokinet* **44:**879-894.

Peters SA, Schroeder PE, Giri N, and Dolgos H (2012) Evaluation of the use of static and dynamic models to predict drug-drug interaction and its associated variability: impact on drug discovery and early development. *Drug Metab Dispos* **40:**1495-1507.

Picard S, Titier K, Etienne G, Teilhet E, Ducint D, Bernard MA, Lassalle R, Marit G, Reiffers J, Begaud B, Moore N, Molimard M, and Mahon FX (2007) Trough imatinib plasma levels are associated with both cytogenetic and molecular responses to standard-dose imatinib in chronic myeloid leukemia. *Blood* **109:**3496-3499.

Proctor NJ, Tucker GT, and Rostami-Hodjegan A (2004) Predicting drug clearance from recombinantly expressed CYPs: intersystem extrapolation factors. *Xenobiotica* **34:**151-178.

Richter T, Murdter TE, Heinkele G, Pleiss J, Tatzel S, Schwab M, Eichelbaum M, and Zanger UM (2004) Potent mechanism-based inhibition of human CYP2B6 by clopidogrel and ticlopidine. *J Pharmacol Exp Ther* **308:**189-197.

Rochat B, Zoete V, Grosdidier A, von Grunigen S, Marull M, and Michielin O (2008) In vitro biotransformation of imatinib by the tumor expressed CYP1A1 and CYP1B1. *Biopharm Drug Dispos* **29:**103-118.

Rostami-Hodjegan A and Tucker GT (2007) Simulation and prediction of in vivo drug metabolism in human populations from in vitro data. *Nat Rev Drug Discov* **6:**140-148.

Rowland Yeo K, Jamei M, Yang J, Tucker GT, and Rostami-Hodjegan A (2010) Physiologically based mechanistic modelling to predict complex drug-drug interactions involving simultaneous competitive and time-dependent enzyme inhibition by parent compound and its metabolite in both liver and gut - the effect of diltiazem on the time-course of exposure to triazolam. *Eur J Pharm Sci* **39:**298-309.

Rowland Yeo K, Walsky RL, Jamei M, Rostami-Hodjegan A, and Tucker GT (2011) Prediction of time-dependent CYP3A4 drug-drug interactions by physiologically based pharmacokinetic modelling: impact of inactivation parameters and enzyme turnover. *Eur J Pharm Sci* **43:**160-173.

Stegmeier F, Warmuth M, Sellers WR, and Dorsch M (2010) Targeted cancer therapies in the twenty-first century: lessons from imatinib. *Clin Pharmacol Ther* **87:**543-552.

Takahashi N, Wakita H, Miura M, Scott SA, Nishii K, Masuko M, Sakai M, Maeda Y, Ishige K, Kashimura M, Fujikawa K, Fukazawa M, Katayama T, Monma F, Narita M, Urase F, Furukawa T, Miyazaki Y, Katayama N, and Sawada K (2010) Correlation between imatinib pharmacokinetics and clinical response in Japanese patients with chronic-phase chronic myeloid leukemia. *Clin Pharmacol Ther* **88:**809-813.

Teng JF, Mabasa VH, and Ensom MH (2012) The role of therapeutic drug monitoring of imatinib in patients with chronic myeloid leukemia and metastatic or unresectable gastrointestinal stromal tumors. *Ther Drug Monit* **34:**85-97.

Tornio A, Niemi M, Neuvonen PJ, and Backman JT (2008) Trimethoprim and the CYP2C8*3 allele have opposite effects on the pharmacokinetics of pioglitazone. *Drug Metab Dispos* **36:**73-80.

Walsky RL, Obach RS, Gaman EA, Gleeson JP, and Proctor WR (2005) Selective inhibition of human cytochrome P4502C8 by montelukast. *Drug Metab Dispos* **33:**413-418.

van Erp NP, Gelderblom H, Karlsson MO, Li J, Zhao M, Ouwerkerk J, Nortier JW, Guchelaar HJ, Baker SD, and Sparreboom A (2007) Influence of CYP3A4 inhibition on the steady-state pharmacokinetics of imatinib. *Clin Cancer Res* **13:**7394-7400.

Wang J, Hughes TP, Kok CH, Saunders VA, Frede A, Groot-Obbink K, Osborn M, Somogyi AA, D'Andrea RJ, and White DL (2012) Contrasting effects of diclofenac and ibuprofen on active imatinib uptake into leukaemic cells. *Br J Cancer* **106**:1772-1778.

Venkatakrishnan K, von Moltke LL, Obach RS, and Greenblatt DJ (2003) Drug metabolism and drug interactions: application and clinical value of in vitro models. *Curr Drug Metab* **4:**423-459.

Footnotes

This work was supported by the Helsinki University Central Hospital Research Fund, Helsinki, Finland. Filppula was also supported by the Clinical Drug Research Graduate School (CDRGS), Helsinki, Finland and the Orion-Farmos Research Foundation, Espoo, Finland

Parts of this work were previously presented at the following conferences:

Anne M. Filppula, Jouko Laitila, Pertti J. Neuvonen, and Janne T. Backman. Contribution of CYP2C8 and CYP3A4 to the main metabolic pathway of imatinib in vitro. 10th EACPT Congress, 2011 June 26-29; Budapest, Hungary.

Anne M. Filppula, Mikko Neuvonen, Jouko Laitila, Pertti J. Neuvonen and Janne T. Backman. Roles of Cytochrome P450 (CYP) 2C8 and CYP3A4 in Imatinib Metabolism – Implications of Autoinhibition of CYP3A4. 19th MDO Meeting and 12th European ISSX Meeting, 2012 June 17–21; Noordwijk aan Zee, the Netherlands.

Reprint requests should be addressed to the corresponding author Prof. Janne T. Backman, Department of Clinical Pharmacology University of Helsinki and HUSLAB, Helsinki University Central Hospital, P.O. Box 705, FI-00029 HUS, FINLAND (E-mail: janne.backman@helsinki.fi).

Figure legends

Fig. 1.

Recombinant P450 isoform and P450 inhibitor screening experiments. A, remaining amount of 0.1 µM and 1 µM imatinib after a 30-min incubation with ten different P450 enzymes (0.5 mg/ml protein). B, initial formation rates of N-DMI in the respective incubations. C, the effects of different P450 isoform inhibitors (concentrations given in Methods) on N-DMI formation rate during incubation of 0.1 µM imatinib with pooled HLM (0.5 mg/ml protein) for 5 min. The inhibitors tested were furafylline (FURA), 8-methoxy-psoralen (8-M-P), clopidogrel (CLOP), gemfibrozil 1-*O*-β glucuronide (GEM-G), montelukast (MONT), sulfaphenazole (SULF), omeprazole (OME), quinidine (QUIN), diethyldithiocarbamate (DDC), ketoconazole (KETO), and troleandomycin (TAO). A 15- or 20-min preincubation of the inhibitor with HLM preceded the incubation in experiments with FURA, 8-M-P, CLOP, GEM-G, DDC, and TAO. Because recombinant CYP1A2, CYP2A6, CYP2B6, and CYP2E1 did not form N-DMI, the observed weak effects of FURA, 8-M-P, CLOP, and QUIN on N-DMI formation in C are likely to be due to nonspecific inhibition of CYP2C8 or CYP3A4 by these compounds. D, the remaining amount of 0.1 µM N-DMI after incubation for 30 min with CYP1A2, CYP2C8, CYP2D6, CYP3A4, CYP3A5, and a P450 mix containing CYP2A6, CYP2B6, CYP2C9, CYP2C19, and CYP2E1 (0.5 mg/ml protein). The equal protein concentrations used in recombinant P450 experiments resulted in variable P450 concentrations in the incubations (see Materials and Methods for exact P450 concentrations). The bars represent mean+SD values of triplicate incubations.

Fig. 2.

Experiments with recombinant P450 enzymes. A, depletion of 0.1 µM imatinib and B, the subsequent formation of N-DMI by CYP2C8, CYP3A4, and CYP3A5. C, the enzyme kinetics of N-DMI formation by CYP2C8, CYP3A4, and CYP3A5. D, depletion of 0.05 µM N-DMI by CYP2C8, CYP3A4, and CYP3A5. The protein concentration was 0.5 mg/ml in all incubations, except in the enzyme kinetic study, where it was 0.1 mg/ml, resulting in variable P450 concentrations in the incubations (see Materials and Methods for exact P450 concentrations). The data points represent mean±SD values of triplicate incubations.

Figure 3

Pharmacokinetic simulations of the single-dose pharmacokinetics of imatinib. A and B, mean simulated and observed imatinib and N-DMI plasma concentrations in 33 healthy volunteers after a single oral dose of imatinib 400 mg. Lines are simulated mean concentration time-profiles of ten trials (dotted lines represent 95% CI:s of the mean), whereas the circles refer to clinical data from Nikolova et al. (2004).

Fig. 4.

Simulated effects of multiple dosing on imatinib pharmacokinetics and enzyme activities. A and B, simulated mean steady-state concentrations of imatinib and N-DMI during administration of imatinib 400 mg daily, when MBI of CYP3A4 by imatinib is included in the model (final model; full line) or when it is excluded from the model (dotted line). C and D, the simulated mean effects of different doses of imatinib on the intestinal and hepatic amounts of active CYP3A4 (as % of initial active amount when treatment is initiated at time 0, and MBI of CYP3A4 is included in the simulation model). E, the simulated importance of CYP2C8 and CYP3A4 in imatinib pharmacokinetics during treatment with imatinib 400 mg once daily (o.d.) or twice daily (b.i.d.). The curves for CYP1A2, CYP2B6, CYP2D6, and CYP3A5 were omitted for clarity, because their roles were negligible (<5% of total hepatic clearance). The simulations were carried out in 100 North European Caucasian subjects.

Fig. 5.

Simulated effects of CYP2C8 polymorphisms and CYP2C8 and CYP3A4 inhibitors on imatinib pharmacokinetics. A and B, simulated steady-state concentrations of imatinib and N-DMI in a typical 60-year old man with different CYP2C8 activities; normal (CYP2C8 reference genotype), 50% decrease (low activity CYP2C8 genotype) or 100% increase (high activity CYP2C8 genotype) in hepatic CYP2C8 activity, after imatinib 400 mg once daily. The line at 1,000 ng/ml in A represents the suggested therapeutic trough concentration of imatinib. C-F, simulation of the effects of a CYP2C8 inhibitor (gemfibrozil) and a CYP3A4 inhibitor (itraconazole) on the pharmacokinetics of imatinib. The simulated effects of a CYP2C8 inhibitor (gemfibrozil 600 mg twice daily), a CYP3A4 inhibitor (itraconazole 100 mg twice daily, except first dose 200 mg) and their combination on imatinib and N-DMI pharmacokinetics after a single dose of imatinib 400 mg on day 3 (C and D) and multiple doses of imatinib 400 mg once daily (E and F), in 30 North European Caucasian subjects.

Tables

Table 1

Enzyme kinetic parameters of imatinib metabolism determined on the basis of recombinant P450 enzyme studies and prediction of the hepatic clearance of imatinib by use of the static ISEF model

P450 isoform	Pathway	CL_{int} (µl/min/pmol)	V_{max} (pmol/min/pmol)	K_m (µM)	$f_{u,mic}$	ISEF[a]	ISEF- and P450 abundance adjusted CL_{int} (µl/min/mg protein)[b]	Scaled CL_{int} (l/h)	CL_H (l/h)	% total CL_H [c]
CYP1A2	Metabolism	0.03	-	-	0.80	BD Sup	0.84	3.6	0.14	1.1
CYP2B6	Metabolism	0.07	-	-	0.80	BD Sup	0.66	2.9	0.11	0.83
CYP2C8	N-DMI	0.95	4.07	4.28	0.90	User	29	127	4.8	40
	Other metabolites	0.14[d]	-	-	[d]	User	3.9	17	0.66	
CYP2D6	Metabolism	0.05	-	-	0.80	BD Sup	0.34	1.5	0.059	0.43
CYP3A4	N-DMI	0.92	13.30	14.40	0.90	User	13	56	2.2	57
	Other metabolites	2.75[d]	-	-	[d]	User	35	151	5.7	
CYP3A5	N-DMI	0.06	4.60	71.50	0.90	User	0.47	2.0	0.081	0.79
	Other metabolites	0.02[d]	-	-	[d]	User	0.16	0.67	0.027	

Abbreviations: $f_{u,mic,}$ unbound fraction of imatinib in microsomal incubations.

[a] Intersystem extrapolation factors used in the Simcyp compound file and in the static model calculations; 'BD Sup' indicates default values within Simcyp for incubations conducted with microsomes from BD Biosciences, whereas 'User' denotes in house values; 1.16 for CYP2C8, 0.09 for CYP3A4, and 0.06 for CYP3A5. Because the P450 activity between different recombinant enzyme lots may vary, in house ISEF factors for the key enzymes in imatinib metabolism were preferred. Furthermore, the best accuracy in interaction predictions was obtained using these values. The in house ISEF factors are based on V_{max} for amodiaquine N-deethylation and midazolam 1'-hydroxylation in recombinant CYP2C8, CYP3A4, CYP3A5, and in pooled HLM.

[b] The average P450 hepatic abundance values used were 52 pmol/mg protein for CYP1A2, 17 pmol/mg protein for CYP2B6, 24 pmol/mg protein for CYP2C8, 8 pmol/mg protein for CYP2D6, 137 pmol/mg protein for CYP3A4, and 103 pmol/mg protein for CYP3A5 (these are average values of the North European Caucasian population within Simcyp).

[c] Calculated contributions of each P450 enzyme to the total hepatic clearance of imatinib.

[d] The unbound fractions of imatinib had previously been determined (Filppula et al., 2012), and vary between 0.8 and 0.9 depending on the protein concentration used in the experiment (0.5 or 0.1 mg/ml, respectively). The CL_{int} values for 'other metabolites' were calculated as the difference between $CL_{int,u,\ ima\ dep}$ and $CL_{int,u,\ N\text{-}DMI\ form}$, and a $f_{u,mic}$ of 1 was entered in Simcyp in this case.

Table 2

Enzyme kinetic parameters N-DMI metabolism determined on the basis of recombinant P450 enzyme studies and prediction of the hepatic clearance of N-DMI by use of the static ISEF model

P450 isoform	Pathway	CL_{int} (µl/min/pmol)	$f_{u,mic}$	ISEF[a]	ISEF- and P450 abundance adjusted CL_{int} (µl/min/mg protein)[b]	Scaled CL_{int} (l/h)	CL_H (l/h)	% total CL_H[c]
CYP1A2	Metabolism	0.03	0.80	BD Sup	0.84	3.6	0.072	4.3
CYP2C8	Metabolism	0.06	0.80	User	2.1	9.2	0.18	11
CYP2D6	Metabolism	0.05	0.80	BD Sup	0.41	1.8	0.035	2.1
CYP3A4	Metabolism	0.50	0.80	User	7.9	34	0.68	40
CYP3A5	Metabolism	0.09	0.80	User	0.76	3.3	0.065	3.9

Abbreviations: $f_{u,mic,}$ unbound fraction of N-DMI in microsomal incubations.

[a] Intersystem extrapolation factors used in the Simcyp compound file and in the static model calculations; 'BD Sup' indicates default values within Simcyp for incubations conducted with microsomes from BD Biosciences, whereas 'User' denotes in house values; 1.16 for CYP2C8, 0.09 for CYP3A4, and 0.06 for CYP3A5. Because the P450 activity between different recombinant enzyme lots may vary, in house ISEF factors for the key enzymes in imatinib metabolism were preferred. Furthermore, the best accuracy in interaction predictions was obtained using these values. The in house ISEF factors are based on V_{max} for amodiaquine N-deethylation and midazolam 1'-hydroxylation in recombinant CYP2C8, CYP3A4, CYP3A5, and in pooled HLM.

[b] The average P450 hepatic abundance values used were 52 pmol/mg protein for CYP1A2, 24 pmol/mg protein for CYP2C8, 8 pmol/mg protein for CYP2D6, 137 pmol/mg protein for CYP3A4, and 103 pmol/mg protein for CYP3A5 (these are average values of the North European Caucasian population within Simcyp). Because the sum of the ISEF- and P450 abundance adjusted CL_{int} values from recombinant P450 enzymes was equivalent to about 60% of the HLM CL_{int} value (20 µl/min/mg), the model for N-DMI in Simcyp also included an additional HLM CL_{int} value of 7.9 µl/min/mg.

[c] Calculated contributions of each P450 enzyme to the total hepatic clearance of N-DMI, assuming that the total CL_H equals 1.7 l/h (calculated based on the HLM CL_{int} value).

Figure 1

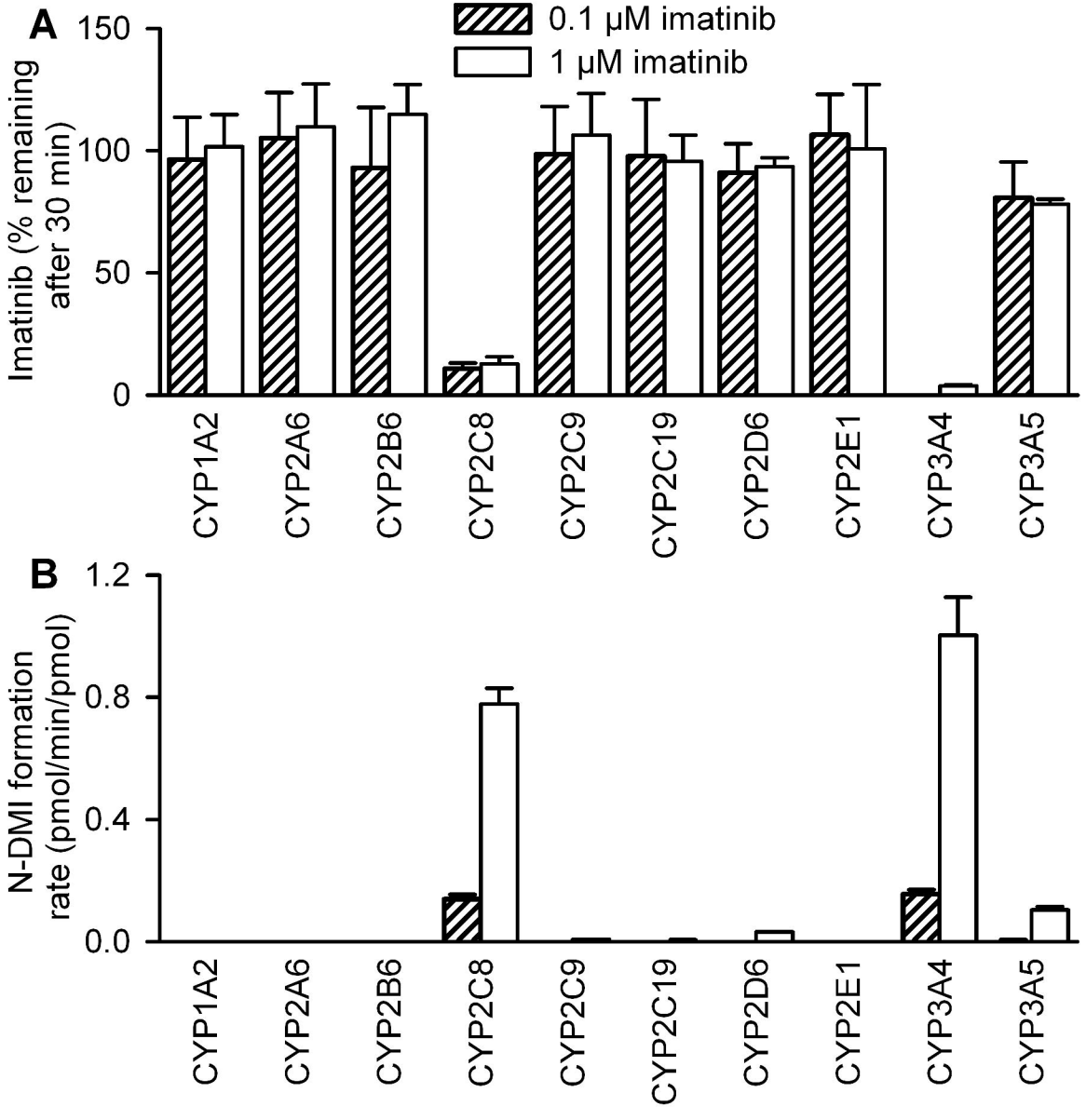

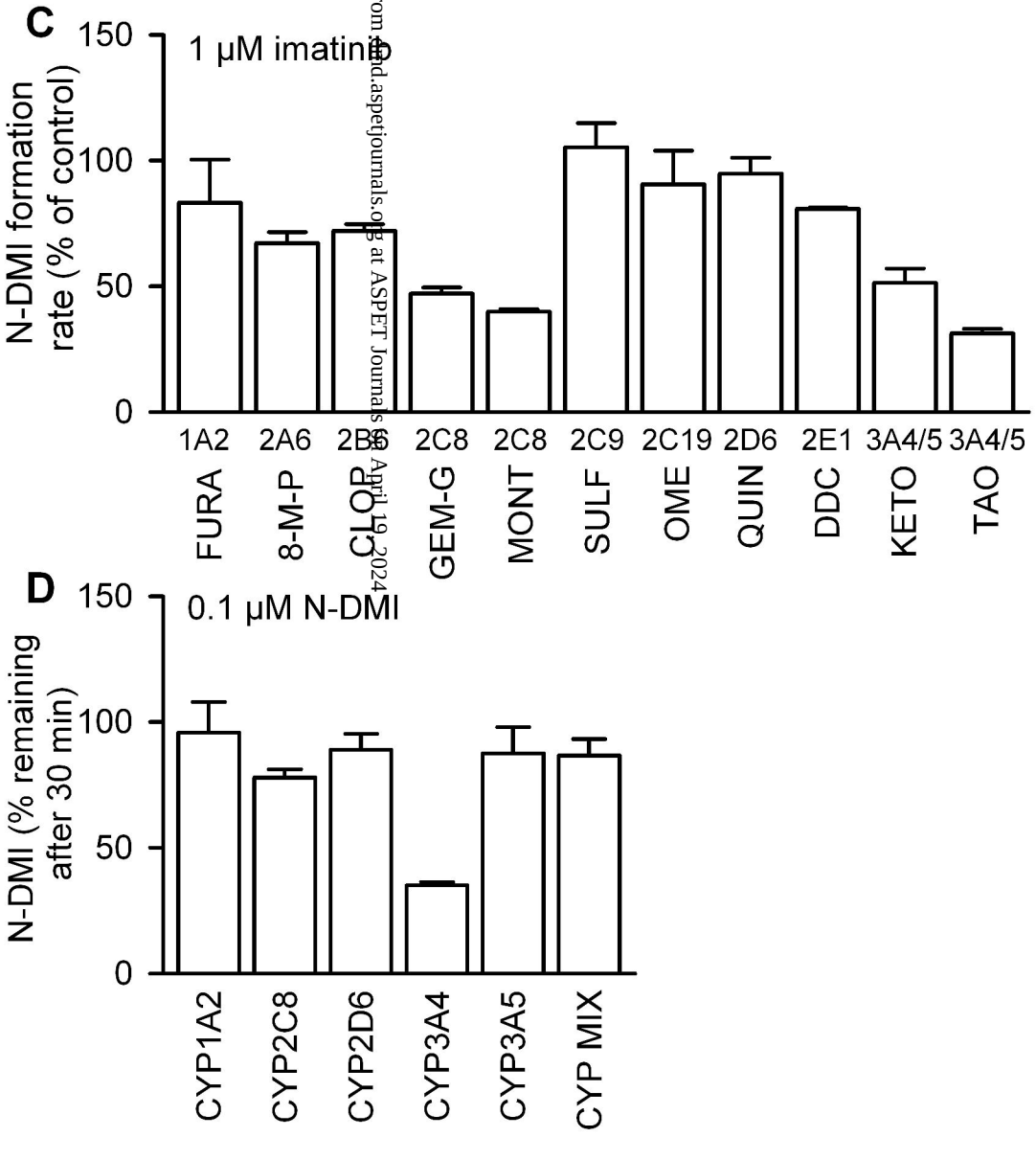

Figure 2

DMD Fast Forward. Published on October 1, 2012 as DOI: 10.1124/dmd.112.048017
This article has not been copyedited and formatted. The final version may differ from this version.

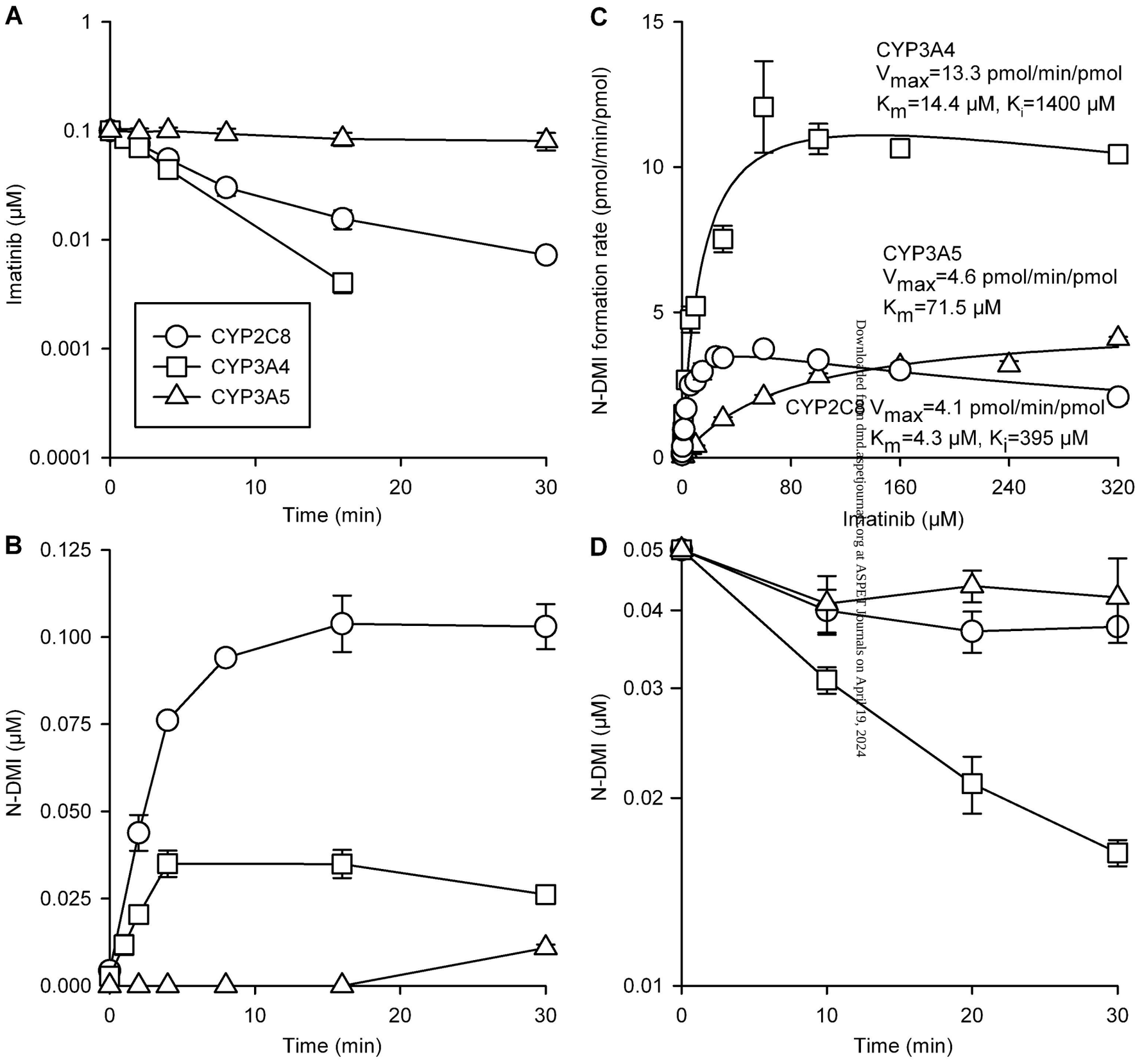

Figure 3

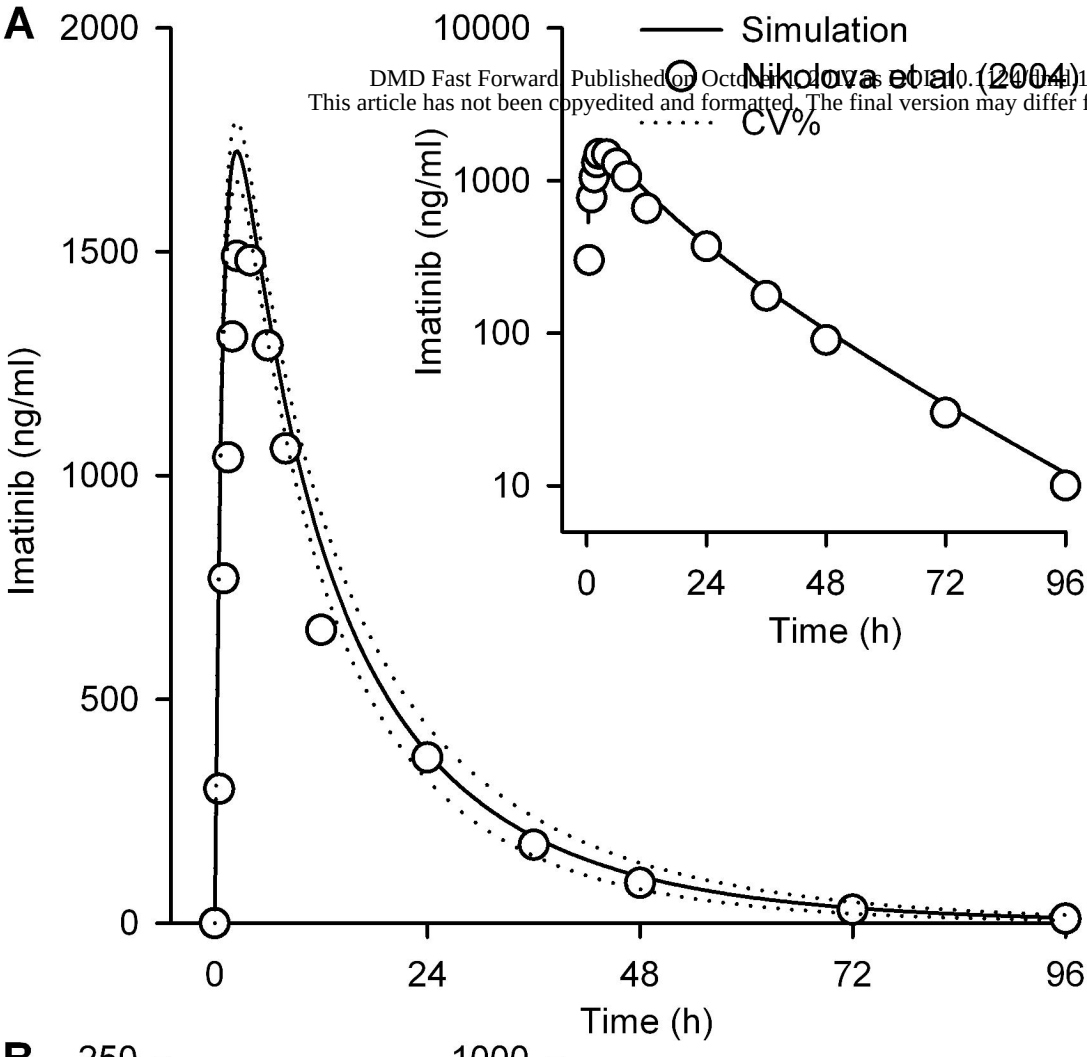

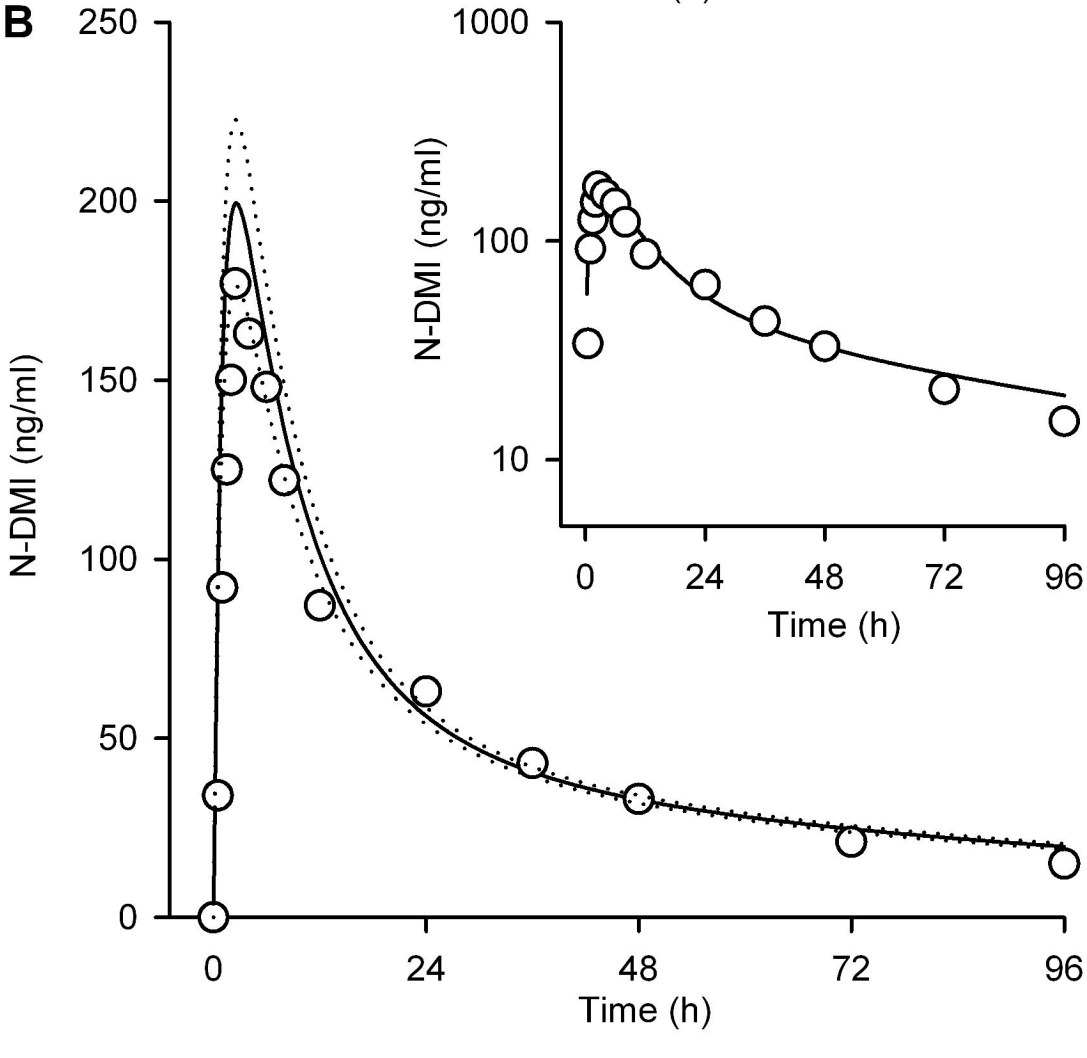

Figure 4

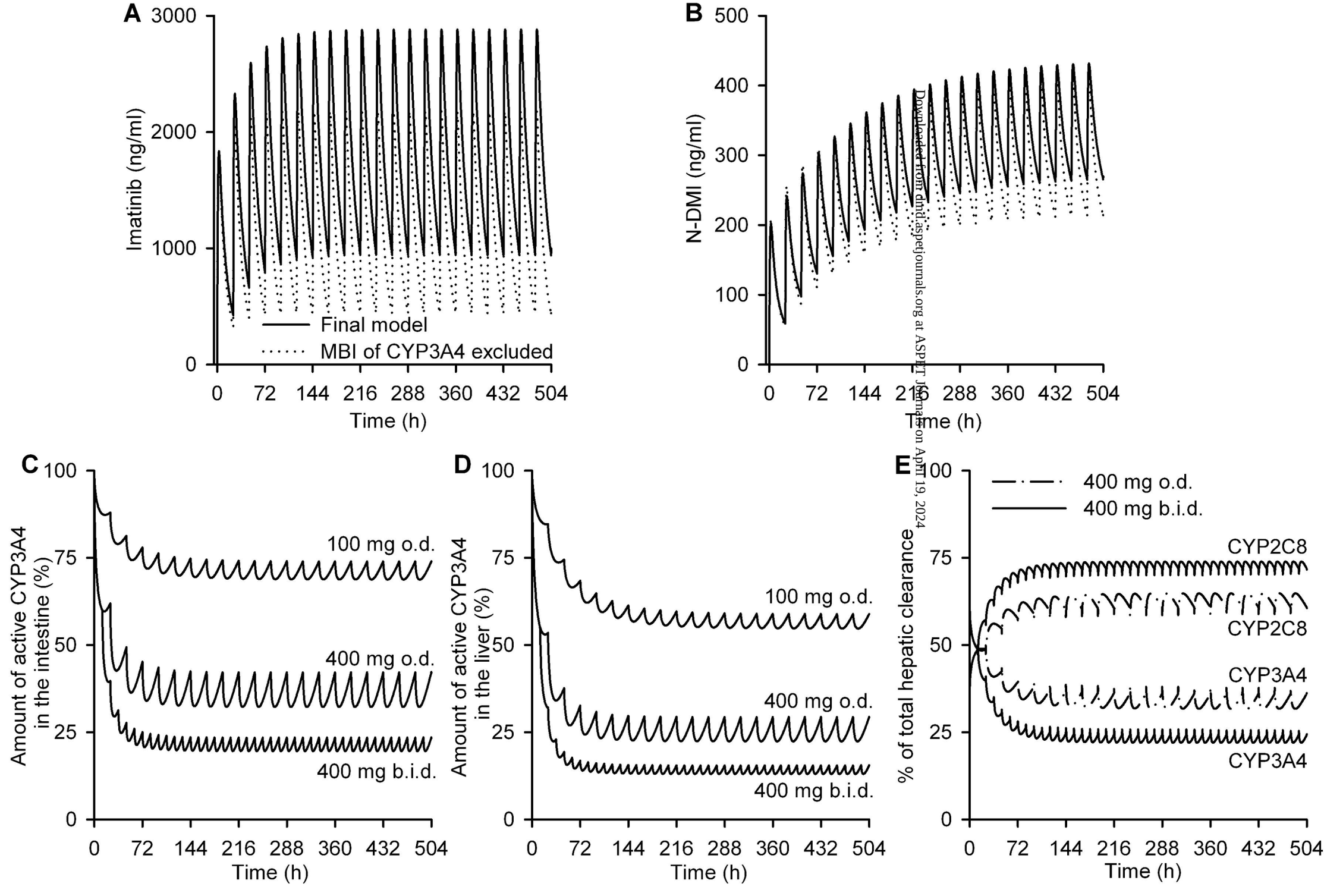

Figure 5

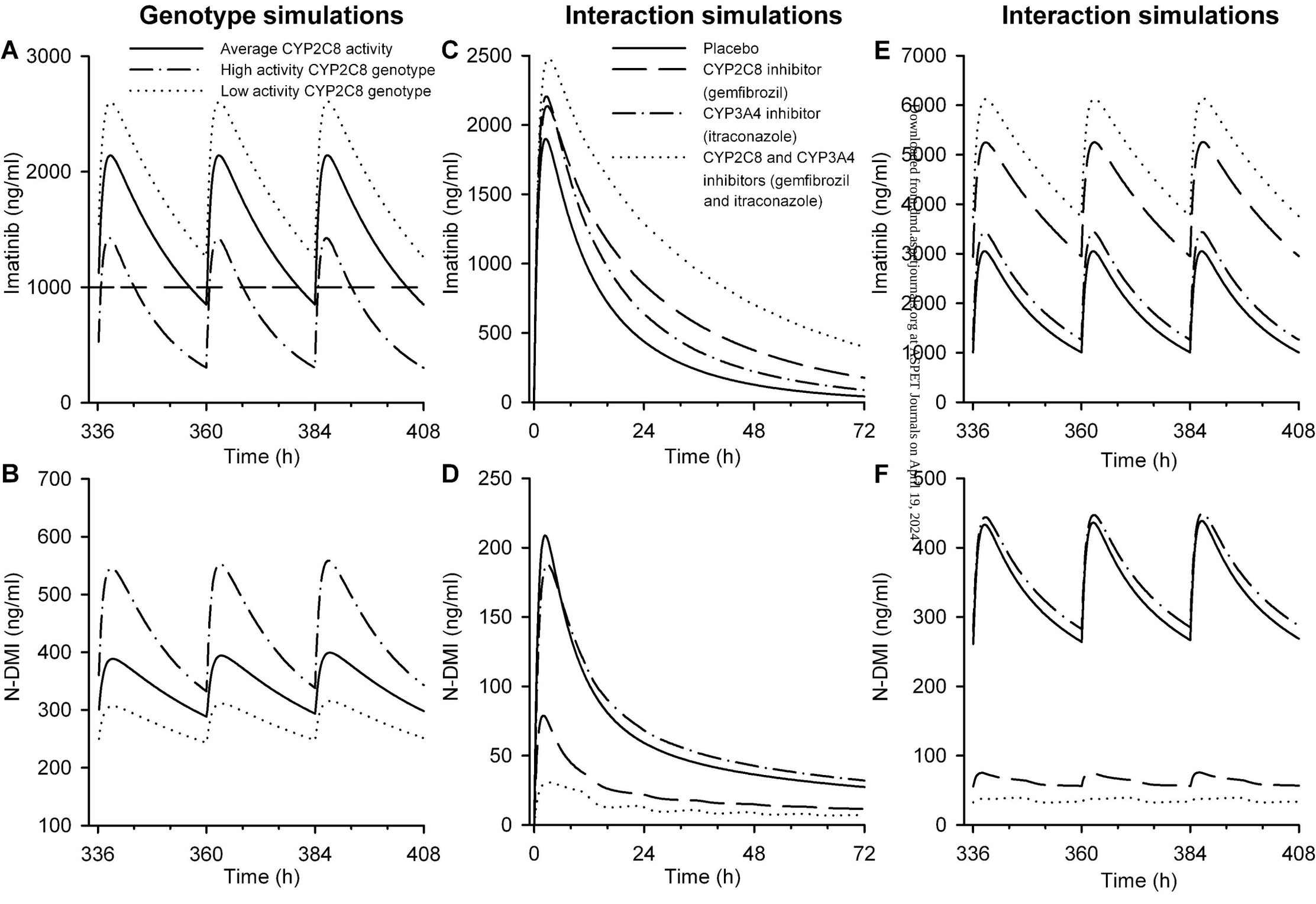

DRUG METABOLISM AND DISPOSITION

SUPPLEMENTARY MATERIAL TO

Autoinhibition of CYP3A4 Leads to Major Role of CYP2C8 in Imatinib Metabolism: Variability in CYP2C8 Activity May Alter Plasma Concentrations and Response

Anne M. Filppula, Mikko Neuvonen, Jouko Laitila, Pertti J. Neuvonen, and Janne T. Backman

Department of Clinical Pharmacology, University of Helsinki, Helsinki, Finland *(A.M.F., M.N., J.L., P.J.N., J.T.B.)* and HUSLAB, Helsinki University Central Hospital, Helsinki, Finland *(P.J.N., J.T.B.)*

Table of Contents:

Supplementary Methods

Details of pharmacokinetic simulations

Seven different simulation studies were carried out. After the final model had been refined by adjusting the additional clearance and the volume of the single adjusting compartment, the plasma concentration-time profiles for imatinib and N-DMI were simulated in ten trials of 33 healthy volunteers after a single dose of imatinib 400 mg for comparison to the reference data from a similar *in vivo* study (Nikolova et al., 2004)(Supplementary Table S3). Thereafter, to validate the model, a steady-state imatinib pharmacokinetic trial was simulated, wherein 100 North European Caucasian subjects (ages 18-75 y, 50% females) received imatinib 100 mg or 400 mg once daily or 400 mg twice daily (Supplementary Table S4). In addition, the model was validated by simulating interactions with ketoconazole, rifampicin and ritonavir (compound files included in Simcyp) in ten trials each, where population and trial parameters were selected according to the corresponding clinical studies (Bolton et al., 2004; Dutreix et al., 2004; van Erp et al., 2007)(Supplementary Table S5).

To translate to our *in vitro* findings to clinical relevance, the effects of CYP2C8 polymorphisms and CYP2C8 and CYP3A4 inhibition on imatinib pharmacokinetics were simulated. To this end, a steady-state imatinib simulation was carried out, wherein a 60-year old North European Caucasian male with different CYP2C8 activities/genotypes (normal, 50% decrease or 100% increase in CYP2C8 abundance in the liver) received imatinib 400 mg once daily. In addition, an interaction trial was simulated, where a single dose of imatinib 400 mg or multiple doses of imatinib 400 mg once daily were given concomitantly with a strong CYP2C8 inhibitor (gemfibrozil; 600 mg twice daily), a strong

CYP3A4 inhibitor (itraconazole; 100 mg twice daily) or their combination, to 30 North European Caucasians (ages 18-75 y, 50% females). The compound file for itraconazole was included in Simcyp, whereas no CYP2C8 inhibitors were available in the software. Therefore, a simple model for gemfibrozil and its 1-*O*-β glucuronide metabolite (a strong mechanism-based CYP2C8 inhibitor) was constructed based on literature data and applied to simulate the interaction trial (Supplementary Tables S6-S8). The compound files included absorption using the compartmental absorption and transition model within Simcyp (for gemfibrozil), intestinal metabolism, a minimal physiologically-based distribution model including a single adjusting compartment, and elimination by renal and hepatic metabolism for gemfibrozil, and by *in vivo* clearance for GEM-G. The model for gemfibrozil and GEM-G was developed for treatment with gemfibrozil 600 mg (Supplementary Fig. S2), and the inhibitory effect on CYP2C8 was validated by comparing interaction simulations, using repaglinide and rosiglitazone as CYP2C8 substrates (included in Simcyp), with published reference data (Niemi et al., 2003a; Niemi et al., 2003b; Tornio et al., 2008)(data not shown).

Supplementary Tables

Supplementary Table S1 Input values of imatinib in the Simcyp compound file, except for the CYP-mediated elimination parameters, which are given in Table 1

Parameter	Value	CV[a]	Notes and references
Physical and chemical properties			
Molecular weight	493.6 g/mol		Imatinib free base (http://www.themerckindex.cambridgesoft.com)
Octanol/water partition coefficient (Log P)	1.99		(Peng et al., 2005)
Compound type	Diprotic base		(Peng et al., 2005)
pKa 1 and 2	8.07, 3.73		(http://www.themerckindex.cambridgesoft.com)
Blood/plasma ratio	0.732		Estimated from (Kretz et al., 2004)
Fraction unbound in plasma (f_u)	0.05		(Peng et al., 2005)
Main plasma binding protein	Alfa-acid-glycoprotein		(http://www.accessdata.fda.gov/drugsatfda_docs/nda/2001/21335_Gleevec.cfm) (Kretz et al., 2004; Peng et al., 2005)
Absorption			
First order absorption model			
Fraction absorbed (f_a)	1	10%	(http://www.accessdata.fda.gov/drugsatfda_docs/nda/2001/21335_Gleevec.cfm) (Peng et al., 2004a)
Absorption rate constant (k_a)	1.1 1/h	10%	Estimated from (http://www.accessdata.fda.gov/drugsatfda_docs/nda/2001/21335_Gleevec.cfm) (Petain et al., 2008)
Free fraction in the enterocytes ($f_{u,gut}$)	0.05		Assumed to correspond to f_u in plasma
Distribution			
Minimal PBPK model			
Volume of distribution at steady-state (V_{ss})	3.5 l/kg	10%	Estimated from literature (Gambacorti-Passerini et al., 2003; le Coutre et al., 2004; Bornhauser et al., 2005; Al-Batran et al., 2007; Treiber et al., 2008)
Single adjusting compartment			
- Clearance into compartment (CL_{in})	1.0 l/h		Estimated
- Clearance out from compartment (CL_{out})	10 l/h		Estimated
- Volume of distribution of compartment (V_{sac})	1.55 l/kg		Estimated
Elimination			
Enzyme kinetic elimination inputs are given in Table 1			
Active uptake into hepatocytes	1		Default value
Renal clearance (CL_R)	0.5 l/h		Estimated from (Bornhauser et al., 2005; Gschwind et al., 2005)
Additional systemic clearance	1.8 l/h	10%	Estimated
Interaction (inhibition of P450 enzymes)			
Inhibition constant K_i (CYP1A2)	410 µM		(http://www.accessdata.fda.gov/drugsatfda_docs/nda/2001/21335_Gleevec.cfm)
K_i (CYP2A6)	230 µM		(http://www.accessdata.fda.gov/drugsatfda_docs/nda/2001/21335_Gleevec.cfm)
K_i (CYP2C8)	8.36 µM		(Filppula et al., 2012)
Unbound fraction in CYP2C8 ($f_{u,mic}$)	0.9		(Filppula et al., 2012)
K_i (CYP2C9)	27 µM		(http://www.accessdata.fda.gov/drugsatfda_docs/nda/2001/21335_Gleevec.cfm)
K_i (CYP2C19)	120 µM		(http://www.accessdata.fda.gov/drugsatfda_docs/nda/2001/21335_Gleevec.cfm)
K_i (CYP2D6)	7.5 µM		(http://www.accessdata.fda.gov/dr

		ugsatfda_docs/nda/2001/21335_Gleevec.cfm)
K_i (CYP3A4)	23.3 µM	(Filppula et al., 2012)
$f_{u,mic}$ (CYP3A4; 0.1 mg/ml)	0.9	(Filppula et al., 2012)
Inhibitor concentration that supports half-maximal rate of inactivation (K_{app})(CYP3A4),	14.3 µM	(Filppula et al., 2012)
Maximal inactivation rate (k_{inact})(CYP3A4)	4.29 pmol/min/pmol,	(Filppula et al., 2012)
$f_{u,mic}$ (CYP3A4; 0.5 mg/ml)	0.8	(Filppula et al., 2012)
K_i (CYP3A5)	23.3 µM	(Filppula et al., 2012)
$f_{u,mic}$ (CYP3A5)	0.9	(Filppula et al., 2012)

[a] The default CV within Simcyp is 30%.

Supplementary Table S2 Input values of N-DMI in the Simcyp compound file, except for the CYP-mediated elimination parameters, which are given in Table 2

Parameter	Value	CV[a]	Notes and references
Physical and chemical properties			
Molecular weight	479.57 g/mol		(http://www.accessdata.fda.gov/drugsatfda_docs/nda/2001/21335_Gleevec.cfm)
Octanol/water partition coefficient (Log P)	1.8		Calculated as imatinib log P x 0.9. The proportion between imatinib and N-DMI log P was estimated from Internet-based log P predictors (http://www.chemaxon.com/products/marvin/marvinsketch/, http://www.molinspiration.com/cgi-bin/properties, https://scifinder.cas.org)
Compound type	Diprotic base		(Peng et al., 2005)
pKa 1 and 2	9.25, 4.66		Estimated from Internet-based pKa predictors (http://www.chemaxon.com/products/marvin/marvinsketch/, https://scifinder.cas.org)
Blood/plasma ratio	0.7725		Estimated from (Kretz et al., 2004)
Fraction unbound in plasma (f_u)	0.03		(Kretz et al., 2004)
Main plasma binding protein	Alfa-acid-glycoprotein		(Kretz et al., 2004)
Absorption			
Free fraction in the enterocytes ($f_{u,gut}$)	0.03		Assumed to correspond to f_u in plasma
Distribution			
Minimal PBPK model			
Volume of distribution at steady-state (V_{ss})	25 l/kg	0%	Estimated from literature assuming that 40% of imatinib is converted to N-DMI
Single adjusting compartment			
- Clearance into compartment (CL_{in})	35 l/h		Estimated
- Clearance out from compartment (CL_{out})	38 l/h		Estimated
- Volume of distribution of compartment (V_{sac})	23.2 l/kg		Estimated
Elimination			
Enzyme kinetic elimination inputs are given in Table 2			
Active uptake into hepatocytes	1		Default value
Renal clearance (CL_R)	1.5 l/h		Estimated
Additional systemic clearance	14 l/h	10%	Estimated
Interaction (inhibition of P450 enzymes)			
Inhibition constant K_i (CYP1A2)	65 µM		(http://www.accessdata.fda.gov/drugsatfda_docs/nda/2001/21335_Gleevec.cfm)
K_i (CYP2C8)	12.8 µM		(Filppula et al., 2012)
Unbound fraction in CYP2C8 ($f_{u,mic}$)	0.9		(Filppula et al., 2012)
K_i (CYP2C9)	40.3 µM		(http://www.accessdata.fda.gov/drugsatfda_docs/nda/2001/21335_Gleevec.cfm)
K_i (CYP2C19)	112 µM		(http://www.accessdata.fda.gov/drugsatfda_docs/nda/2001/21335_Gleevec.cfm)
K_i (CYP2D6)	13.5 µM		(http://www.accessdata.fda.gov/drugsatfda_docs/nda/2001/21335_Gleevec.cfm)
K_i (CYP3A4)	18.1 µM		(Filppula et al., 2012)
$f_{u,mic}$ (CYP3A4)	0.9		(Filppula et al., 2012)
K_i (CYP3A5)	18.1 µM		(Filppula et al., 2012)
$f_{u,mic}$ (CYP3A5)	0.9		(Filppula et al., 2012)

[a] The default CV within Simcyp is 30%.

Supplementary Table S3 Simulated and literature pharmacokinetic variables of imatinib and N-DMI in 33 healthy volunteers[a] after a single oral dose of imatinib 400 mg

Compound	Variable	Simulation Mean values (range) of ten simulated trials	Nikolova et al. (2004) Mean values (±SD) or median with range (for t_{max})
Imatinib	t_{max} (h)	2.5 (2.3-2.5)	2.5 (1.5-6.0)
	C_{max} (ng/ml)	1725 (1625-1852)	1606 (±647)
	AUC_{0-96} (ng·h/ml)	29108 (25510-35301)	25150 (±11611)
N-DMI	t_{max} (h)	2.6 (2.5-2.8)	2.5 (1.5-6)
	C_{max} (ng/ml)	199 (150-233)	186 (±72)
	AUC_{0-96} (ng·h/ml)	4875 (4282-5342)	4505 (±1785)

Abbreviations: t_{max}, time to C_{max}, C_{max}, peak concentration.
[a] Ages 18-65 y, fraction of females=0.18.

Supplementary Table S4 Simulated pharmacokinetic data following multiple doses of imatinib in a North European Caucasian population (n=100)[a] and mean pharmacokinetic data in patient populations from the literature

Imatinib dose	Compound	Mean simulation results (CV), day 30			Mean literature data (CV), steady-state			Reference
		C_0 (ng/ml)	C_{max} (ng/ml)	AUC_{0-24} (ng·h/ml)	C_0 (ng/ml)	C_{max} (ng/ml)	AUC_{0-24} (ng·h/ml)	
100 mg o.d.	Imatinib	166 (90%)	626 (38%)	8672 (55%)	N/A	652 (32%)	11400 (37%)	(Gibbons et al., 2008)
	N-DMI	61 (30%)	109 (34%)	1956 (30%)	N/A	139 (32%)	2570 (36%)	
400 mg o.d.	Imatinib	937 (78%)	2889 (37%)	43375 (51%)	910-1530 (44%-64%)	2200-3405 (30%-42%)	33000-56400 (37%-43%)	(Peng et al., 2004b; Peng and Capdeville, 2005; Picard et al., 2007; van Erp et al., 2007; Gibbons et al., 2008; Larson et al., 2008; Demetri et al., 2009; Forrest et al., 2009; Takahashi et al., 2010; Kim et al., 2011)
	N-DMI	269 (29%)	438 (36%)	8309 (31%)	170-301 (44%-54%)	290-556 (32%-37%)	5000-10280 (36%-45%)	
400 mg b.i.d.	Imatinib	2998 (60%)	4790 (42%)	94900 (49%)	2660-2737 (43-47%)	3702 (39%)	68400 (30%)	(Peng et al., 2004b; Peng and Capdeville, 2005; Guilhot et al., 2012)
	N-DMI	623 (31%)	760 (35%)	16730 (33%)	522 (51%)	665 (41%)	13200 (43%)	

Abbreviations: C_0, trough concentration, C_{max}, peak concentration, o.d., once daily, b.i.d., twice daily, N/A, not available.

[a] Trial design: imatinib 100 mg once daily, 400 mg once daily, or 400 mg twice daily were given to 100 North European Caucasian subjects (ages 18-75 y, female fraction=0.50, 1 trial). North European Caucasians were assumed to represent a real patient population better than healthy volunteers.

Supplementary Table S5 Comparison of simulated studies[a] to published studies on the effects of ketoconazole, rifampicin, and ritonavir on the pharmacokinetics of imatinib

Study description	Imatinib dose	Inhibitor/inducer dose	Simulation population parameters	Simulated results and reference data			Reference study
				Compound	Simulated mean (range) change in AUC_{0-24}[b] (ratio-to-control) of ten trials	Literature mean change in AUC_{0-24}[b] (ratio-to-control), one trial	
Interaction study with ketoconazole[b]	200 mg, single dose	400 mg, single dose	Healthy volunteers, n=14, ages 35-59 y, $f_{females}$=0.07	Imatinib	1.44 (1.31-1.59)	1.40	(Dutreix et al., 2004)
				N-DMI	0.98 (0.89-1.08)	0.86	
Interaction study with rifampicin[b, c]	400 mg, single dose on day 5	600 mg o.d. on days 1-8	Healthy volunteers, n=14, ages 40-64 y, $f_{females}$=0.07	Imatinib	0.37 (0.31-0.44)	0.33	(Bolton et al., 2004)
				N-DMI	1.47 (1.35-1.61)	1.26	
Interaction study with ritonavir[b]	400 mg o.d. on days 1-32[d]	600 mg o.d., 30 min before imatinib on days 30-32	NEurCaucasians[e], n=11, ages 51-79 y, $f_{females}$=0.45	Imatinib	1.07 (0.99-1.13)[f]	0.97[f]	(van Erp et al., 2007)
				N-DMI	1.01 (0.99-1.04)[f]	1.39[f]	

Abbreviations: f_{female}, fraction of females.

[a] Each simulation study was carried out in 10 trials.

[b] The compound files for these inhibitors/inducers are included within the Simcyp simulator.

[c] The Simcyp compound file for rifampicin was modified so that induction of CYP2C8 by rifampicin was included in the model. A maximal induction value of 6.27 was added to the compound file of rifampicin. This value was calculated with the Simcyp calculator based on induction data of CYP2C8 and CYP3A4 by rifampicin reported in (Raucy et al., 2002).

[d] In the clinical study, subjects had received imatinib treatment for at least two months prior to the interaction study. However, due to computer capacity limitations the simulated subjects received ritonavir on imatinib treatment day 30. Furthermore, in the clinical setting, the imatinib dose was reduced by 50% during coadministration of ritonavir. Because this modification was not possible within the software, the subjects received imatinib 400 mg also during coadministration.

[e] North European Caucasians were used in the simulation, because the reference data were for a patient population.

[f] The published ritonavir study ratios are geometric means. Thus, geometric mean ratios were calculated for each of the simulated ten trials and the mean values (ratio) of these are shown in the table.

Supplementary Table S6 Input values of gemfibrozil in the Simcyp compound file

Parameter	Value	CV[a]	Notes and references
Physical and chemical properties			
Molecular weight	250.33 g/mol		(http://www.themerckindex.cambridgesoft.com, https://scifinder.cas.org)
Octanol/water partition coefficient (Log P)	4.302		(https://scifinder.cas.org)
Compound type	Monoprotic acid		(https://scifinder.cas.org)
pKa 1	4.75		(https://scifinder.cas.org)
Blood/plasma ratio	0.75		(Gill et al., 2012)
Fraction unbound in plasma (f_u)	0.005		(Gill et al., 2012)
Main plasma binding protein	Albumin		(Hamberger et al., 1986)
Absorption			
Compartmental absorption and transit model			
Free fraction in the enterocytes ($f_{u,gut}$)	0.005		Assumed to correspond to f_u in plasma
Effective permeability in man ($P_{eff,man}$)	$4.62 \cdot 10^{-4}$ cm/s		Predicted within Simcyp on the basis of PSA and HBD values of gemfibrozil
Polar surface area (PSA)	46.5 $Å^2$		(https://scifinder.cas.org)
Number of hydrogen bond donors (HBD)	1		(https://scifinder.cas.org)
Distribution			
Minimal PBPK model			
Volume of distribution at steady-state (V_{ss})	0.13 l/kg	30%	(http://www.pfizer.com/files/products/uspi_lopid.pdf)
Single adjusting compartment			
- Clearance into compartment (CL_{in})	3.0 l/h		Estimated
- Clearance out from compartment (CL_{out})	0.05 l/h		Estimated
- Volume of distribution of compartment (V_{sac})	0.02 l/kg		Estimated
Active uptake into hepatocytes	1		Default value
Elimination			
Clearance type: Enzyme kinetics			
- Pathway 1: GEM-G (UGT2B7), V_{max}, K_m	353 pmol/min/mg, 2.2 µM		(Mano et al., 2007)
- Additional HLM CL_{int}	26.7 µl/min/mg	30%	(Cubitt et al., 2009)
- Additional HIM CL_{int}	1.1 µl/min/mg	30%	(Cubitt et al., 2009)
Renal clearance (CL_R)	0.1 l/h		(Gill et al., 2012)
Additional systemic clearance	2 l/h	30%	Estimated
Interaction (inhibition of P450 enzymes)			
Inhibition constant K_i (CYP1A2)	82 µM		(Wen et al., 2001)
K_i (CYP2C8)	30.4 µM		(Kajosaari et al., 2005)
K_i (CYP2C9)	5.8 µM		(Wen et al., 2001)
K_i (CYP2C19)	24 µM		(Wen et al., 2001)

[a] The default CV within Simcyp is 30%.

Supplementary Table S7 Input values of GEM-G in the Simcyp compound file

Parameter	Value	CV[a]	Notes and references
Physical and chemical properties			
Molecular weight	426.459		(http://www.chemaxon.com/products/marvin/marvinsketch/, https://scifinder.cas.org)
Octanol/water partition coefficient (Log P)	3.304		(https://scifinder.cas.org)
Compound type	Monoprotic acid		(https://scifinder.cas.org)
pKa 1	2.68		
Blood/plasma ratio	1		Default value
Fraction unbound in plasma (f_u)	0.11		(Shitara et al., 2004)
Main plasma binding protein	Albumin		Estimated
Free fraction in the enterocytes ($f_{u,gut}$)	0.11		Assumed to correspond to f_u in plasma
Distribution			
Minimal PBPK model			
Volume of distribution at steady-state (V_{ss})	0.3 l/kg	5%	Estimated
Single adjusting compartment			
- Clearance into compartment (CL_{in})	1.0 1/h		Estimated
- Clearance out from compartment (CL_{out})	0.1 1/h		Estimated
- Volume of distribution of compartment (V_{sac})	0.25 l/kg		Estimated
Elimination			
In vivo clearance			
Active uptake into hepatocytes	1		Default value
Clearance type: In vivo clearance			
- Peroral clearance	3 l/h	30%	Estimated
Interaction (inhibition of P450 enzymes)			
K_{app} (CYP2C8)	20 µM		(Ogilvie et al., 2006)
k_{inact} (CYP2C8)	12.6 1/h		(Ogilvie et al., 2006)

[a] The default CV within Simcyp is 30%.

Supplementary Table S8 Simulated effects of gemfibrozil and/or itraconazole on the pharmacokinetics of imatinib in North European Caucasian subjects (n=30)[a]

Pretreatment	Compound	C_0 ratio to control (95% CI)	C_{max} ratio to control (95% CI)		AUC_{0-24} ratio to control (95% CI)	$AUC_{0-\infty}$ ratio to control (95% CI)	$AUC_{0-\tau}$ ratio to control (95% CI)
		Multiple[b]	Single[b]	Multiple[b]	Single[b]	Single[b]	Multiple[b]
Gemfibrozil	Imatinib	3.75 (2.79-5.05)	1.13 (1.10-1.17)	1.74 (1.59-1.91)	1.66 (1.47-1.87)	1.77 (1.56-2.02)	2.25 (1.93-2.62)
	N-DMI	0.19 (0.15-0.24)	0.35 (0.29-0.42)	0.15 (0.11-0.19)	0.35 (0.29-0.42)	0.41 (0.36-0.48)	0.16 (0.12-0.21)
Itraconazole[c]	Imatinib	1.35 (1.24-1.47)	1.14 (1.12-1.17)	1.12 (1.09-1.16)	1.35 (1.29-1.42)	1.38 (1.31-1.45)	1.18 (1.13-1.24)
	N-DMI	1.09 (1.06-1.12)	0.85 (0.80-0.89)	1.03 (1.01-1.04)	1.07 (1.04-1.10)	1.06 (0.40-2.80)	1.06 (1.04-1.09)
Gemfibrozil and itraconazole[c]	Imatinib	5.27 (3.71-7.48)	1.32 (1.26-1.38)	2.08 (1.89-2.30)	2.51 (2.19-2.89)	2.94 (2.55-3.40)	2.84 (2.41-3.35)
	N-DMI	0.08 (0.06-0.12)	0.11 (0.08-0.15)	0.06 (0.04-0.08)	0.15 (0.11-0.21)	0.21 (0.16-0.27)	0.07 (0.05-0.10)

Abbreviations: C_0, trough concentration, C_{max}, peak concentration, CI, confidence interval

Values shown are geometric means. In addition, 95% confidence intervals for the ratio relative to the control are shown.

[a] Trial design: the effects of gemfibrozil (strong CYP2C8 inhibitor; 600 mg twice daily), or itraconazole (strong CYP3A4 inhibitor; 100 mg twice daily, except first dose 200 mg), or a combination of gemfibrozil and itraconazole on the pharmacokinetics of imatinib (on day 3: 400 mg single dose, or 400 mg once daily 1h after pretreatment) were simulated in a North European population (n=30, ages 18-75 y, $f_{females}$=0.50). North European Caucasians were assumed to represent a real patient population better than healthy volunteers.

[b] Single or multiple doses of imatinib.

[c] The compound file for itraconazole is included in Simcyp; the simulations did not consider inhibition of CYP3A4 by its OH-metabolite.

Supplementary Figure

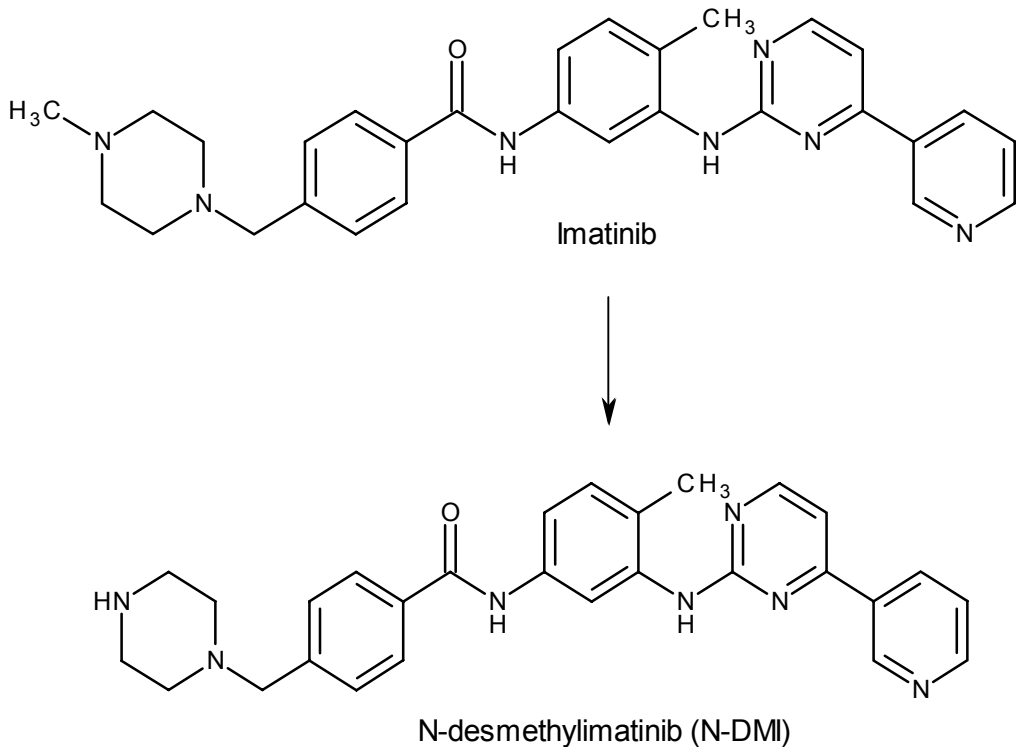

Supplementary Fig. S1.

Chemical structures of imatinib and its pharmacologically active main metabolite N-desmethylimatinib.

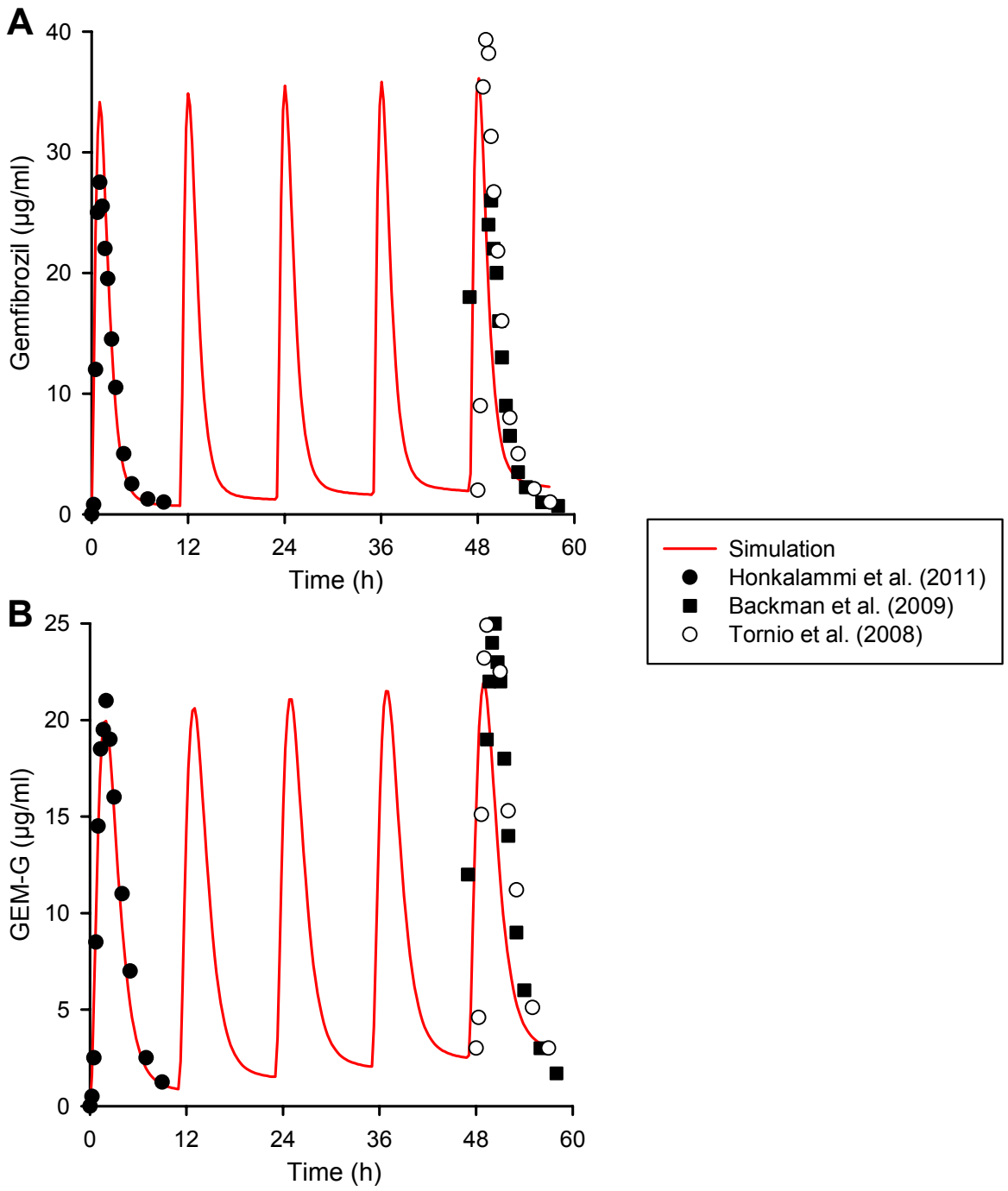

Supplementary Fig. S2.

Simulations of the pharmacokinetics of gemfibrozil and GEM-G. A and B, mean simulated gemfibrozil and GEM-G plasma concentrations in 30 North European Caucasians after administration of gemfibrozil 600 mg twice daily (lines), and corresponding observed data from Honkalammi et al. (2011)(filled circles) Backman et al. (2009)(filled squares), and Tornio et al. (2008)(open circles).

Supplement References

Al-Batran SE, Atmaca A, Schleyer E, Pauligk C, Hosius C, Ehninger G, and Jager E (2007) Imatinib mesylate for targeting the platelet-derived growth factor beta receptor in combination with fluorouracil and leucovorin in patients with refractory pancreatic, bile duct, colorectal, or gastric cancer--a dose-escalation Phase I trial. *Cancer* **109:**1897-1904.

Backman JT, Honkalammi J, Neuvonen M, Kurkinen KJ, Tornio A, Niemi M, and Neuvonen PJ (2009) CYP2C8 activity recovers within 96 hours after gemfibrozil dosing: estimation of CYP2C8 half-life using repaglinide as an in vivo probe. *Drug Metab Dispos* **37:**2359-2366.

Bolton AE, Peng B, Hubert M, Krebs-Brown A, Capdeville R, Keller U, and Seiberling M (2004) Effect of rifampicin on the pharmacokinetics of imatinib mesylate (Gleevec, STI571) in healthy subjects. *Cancer Chemother Pharmacol* **53:**102-106.

Bornhauser M, Pursche S, Bonin M, Freiberg-Richter J, Jenke A, Illmer T, Ehninger G, and Schleyer E (2005) Elimination of imatinib mesylate and its metabolite N-desmethyl-imatinib. *J Clin Oncol* **23:**3855-3856; author reply 3857-3858.

Cubitt HE, Houston JB, and Galetin A (2009) Relative importance of intestinal and hepatic glucuronidation-impact on the prediction of drug clearance. *Pharm Res* **26:**1073-1083.

Demetri GD, Wang Y, Wehrle E, Racine A, Nikolova Z, Blanke CD, Joensuu H, and von Mehren M (2009) Imatinib plasma levels are correlated with clinical benefit in patients with unresectable/metastatic gastrointestinal stromal tumors. *J Clin Oncol* **27:**3141-3147.

Dutreix C, Peng B, Mehring G, Hayes M, Capdeville R, Pokorny R, and Seiberling M (2004) Pharmacokinetic interaction between ketoconazole and imatinib mesylate (Glivec) in healthy subjects. *Cancer Chemother Pharmacol* **54:**290-294.

Filppula AM, Laitila J, Neuvonen PJ, and Backman JT (2012) Potent mechanism-based inhibition of CYP3A4 by imatinib explains its liability to interact with CYP3A4 substrates. *Br J Pharmacol* **165:**2787-2798.

Forrest DL, Trainor S, Brinkman RR, Barnett MJ, Hogge DE, Nevill TJ, Shepherd JD, Nantel SH, Toze CL, Sutherland HJ, Song KW, Lavoie JC, Power MM, Abou-Mourad Y, and Smith CA (2009) Cytogenetic and molecular responses to standard-dose imatinib in chronic myeloid leukemia are correlated with Sokal risk scores and duration of therapy but not trough imatinib plasma levels. *Leuk Res* **33:**271-275.

Gambacorti-Passerini C, Zucchetti M, Russo D, Frapolli R, Verga M, Bungaro S, Tornaghi L, Rossi F, Pioltelli P, Pogliani E, Alberti D, Corneo G, and D'Incalci M (2003) Alpha1 acid glycoprotein binds to imatinib (STI571) and substantially alters its pharmacokinetics in chronic myeloid leukemia patients. *Clin Cancer Res* **9:**625-632.

Gibbons J, Egorin MJ, Ramanathan RK, Fu P, Mulkerin DL, Shibata S, Takimoto CH, Mani S, LoRusso PA, Grem JL, Pavlick A, Lenz HJ, Flick SM, Reynolds S, Lagattuta TF, Parise RA, Wang Y, Murgo AJ, Ivy SP, and Remick SC (2008) Phase I and pharmacokinetic study of imatinib mesylate in patients with advanced malignancies and varying degrees of renal dysfunction: a study by the National Cancer Institute Organ Dysfunction Working Group. *J Clin Oncol* **26:**570-576.

Gill KL, Houston JB, and Galetin A (2012) Characterization of in vitro glucuronidation clearance of a range of drugs in human kidney microsomes: comparison with liver and intestinal glucuronidation and impact of albumin. *Drug Metab Dispos* **40:**825-835.

Gschwind HP, Pfaar U, Waldmeier F, Zollinger M, Sayer C, Zbinden P, Hayes M, Pokorny R, Seiberling M, Ben-Am M, Peng B, and Gross G (2005) Metabolism and disposition of imatinib mesylate in healthy volunteers. *Drug Metab Dispos* **33:**1503-1512.

Guilhot F, Hughes TP, Cortes J, Druker BJ, Baccarani M, Gathmann I, Hayes M, Granvil C, and Wang Y (2012) Plasma exposure of imatinib and its correlation with clinical response in the Tyrosine Kinase Inhibitor Optimization and Selectivity Trial. *Haematologica* **97:**731-738.

Hamberger C, Barre J, Zini R, Taiclet A, Houin G, and Tillement JP (1986) In vitro binding study of gemfibrozil to human serum proteins and erythrocytes: interactions with other drugs. *Int J Clin Pharmacol Res* **6:**441-449.

Honkalammi J, Niemi M, Neuvonen PJ, and Backman JT (2011) Mechanism-based inactivation of CYP2C8 by gemfibrozil occurs rapidly in humans. *Clin Pharmacol Ther* **89:**579-586.

Kajosaari LI, Laitila J, Neuvonen PJ, and Backman JT (2005) Metabolism of repaglinide by CYP2C8 and CYP3A4 in vitro: effect of fibrates and rifampicin. *Basic Clin Pharmacol Toxicol* **97:**249-256.

Kim DW, Tan EY, Jin Y, Park S, Hayes M, Demirhan E, Schran H, and Wang Y (2011) Effects of imatinib mesylate on the pharmacokinetics of paracetamol (acetaminophen) in Korean patients with chronic myelogenous leukaemia. *Br J Clin Pharmacol* **71:**199-206.

Kretz O, Weiss HM, Schumacher MM, and Gross G (2004) In vitro blood distribution and plasma protein binding of the tyrosine kinase inhibitor imatinib and its active metabolite, CGP74588, in rat, mouse, dog, monkey, healthy humans and patients with acute lymphatic leukaemia. *Br J Clin Pharmacol* **58:**212-216.

Larson RA, Druker BJ, Guilhot F, O'Brien SG, Riviere GJ, Krahnke T, Gathmann I, and Wang Y (2008) Imatinib pharmacokinetics and its correlation with response and safety in chronic-phase chronic myeloid leukemia: a subanalysis of the IRIS study. *Blood* **111:**4022-4028.

le Coutre P, Kreuzer KA, Pursche S, Bonin M, Leopold T, Baskaynak G, Dorken B, Ehninger G, Ottmann O, Jenke A, Bornhauser M, and Schleyer E (2004) Pharmacokinetics and cellular uptake of imatinib and its main metabolite CGP74588. *Cancer Chemother Pharmacol* **53:**313-323.

Mano Y, Usui T, and Kamimura H (2007) The UDP-glucuronosyltransferase 2B7 isozyme is responsible for gemfibrozil glucuronidation in the human liver. *Drug Metab Dispos* **35:**2040-2044.

Niemi M, Backman JT, Granfors M, Laitila J, Neuvonen M, and Neuvonen PJ (2003a) Gemfibrozil considerably increases the plasma concentrations of rosiglitazone. *Diabetologia* **46:**1319-1323.

Niemi M, Backman JT, Neuvonen M, and Neuvonen PJ (2003b) Effects of gemfibrozil, itraconazole, and their combination on the pharmacokinetics and pharmacodynamics of repaglinide: potentially hazardous interaction between gemfibrozil and repaglinide. *Diabetologia* **46:**347-351.

Nikolova Z, Peng B, Hubert M, Sieberling M, Keller U, Ho YY, Schran H, and Capdeville R (2004) Bioequivalence, safety, and tolerability of imatinib tablets compared with capsules. *Cancer Chemother Pharmacol* **53:**433-438.

Ogilvie BW, Zhang D, Li W, Rodrigues AD, Gipson AE, Holsapple J, Toren P, and Parkinson A (2006) Glucuronidation converts gemfibrozil to a potent, metabolism-dependent inhibitor of CYP2C8: implications for drug-drug interactions. *Drug Metab Dispos* **34:**191-197.

Peng B and Capdeville R (2005) In Reply. *Journal of Clinical Oncology* **23:**3857-3858.

Peng B, Dutreix C, Mehring G, Hayes MJ, Ben-Am M, Seiberling M, Pokorny R, Capdeville R, and Lloyd P (2004a) Absolute bioavailability of imatinib (Glivec) orally versus intravenous infusion. *J Clin Pharmacol* **44:**158-162.

Peng B, Hayes M, Resta D, Racine-Poon A, Druker BJ, Talpaz M, Sawyers CL, Rosamilia M, Ford J, Lloyd P, and Capdeville R (2004b) Pharmacokinetics and pharmacodynamics of imatinib in a phase I trial with chronic myeloid leukemia patients. *J Clin Oncol* **22:**935-942.

Peng B, Lloyd P, and Schran H (2005) Clinical pharmacokinetics of imatinib. *Clin Pharmacokinet* **44:**879-894.

Petain A, Kattygnarath D, Azard J, Chatelut E, Delbaldo C, Geoerger B, Barrois M, Seronie-Vivien S, LeCesne A, and Vassal G (2008) Population pharmacokinetics and pharmacogenetics of imatinib in children and adults. *Clin Cancer Res* **14:**7102-7109.

Picard S, Titier K, Etienne G, Teilhet E, Ducint D, Bernard MA, Lassalle R, Marit G, Reiffers J, Begaud B, Moore N, Molimard M, and Mahon FX (2007) Trough imatinib plasma levels are associated with both cytogenetic and molecular responses to standard-dose imatinib in chronic myeloid leukemia. *Blood* **109:**3496-3499.

Raucy JL, Mueller L, Duan K, Allen SW, Strom S, and Lasker JM (2002) Expression and induction of CYP2C P450 enzymes in primary cultures of human hepatocytes. *J Pharmacol Exp Ther* **302:**475-482.

Shitara Y, Hirano M, Sato H, and Sugiyama Y (2004) Gemfibrozil and its glucuronide inhibit the organic anion transporting polypeptide 2 (OATP2/OATP1B1:SLC21A6)-mediated hepatic uptake and CYP2C8-mediated metabolism of cerivastatin: analysis of the mechanism of the clinically relevant drug-drug interaction between cerivastatin and gemfibrozil. *J Pharmacol Exp Ther* **311:**228-236.

Takahashi N, Wakita H, Miura M, Scott SA, Nishii K, Masuko M, Sakai M, Maeda Y, Ishige K, Kashimura M, Fujikawa K, Fukazawa M, Katayama T, Monma F, Narita M, Urase F, Furukawa T, Miyazaki Y, Katayama N, and Sawada K (2010) Correlation between imatinib pharmacokinetics and clinical response in Japanese patients with chronic-phase chronic myeloid leukemia. *Clin Pharmacol Ther* **88:**809-813.

Tornio A, Niemi M, Neuvonen M, Laitila J, Kalliokoski A, Neuvonen PJ, and Backman JT (2008) The effect of gemfibrozil on repaglinide pharmacokinetics persists for at least 12 h after the dose: evidence for mechanism-based inhibition of CYP2C8 in vivo. *Clin Pharmacol Ther* **84:**403-411.

Treiber G, Wex T, Schleyer E, Troeger U, Hosius C, and Malfertheiner P (2008) Imatinib for hepatocellular cancer--focus on pharmacokinetic/pharmacodynamic modelling and liver function. *Cancer Lett* **260:**146-154.

van Erp NP, Gelderblom H, Karlsson MO, Li J, Zhao M, Ouwerkerk J, Nortier JW, Guchelaar HJ, Baker SD, and Sparreboom A (2007) Influence of CYP3A4 inhibition on the steady-state pharmacokinetics of imatinib. *Clin Cancer Res* **13:**7394-7400.

Wen X, Wang JS, Backman JT, Kivisto KT, and Neuvonen PJ (2001) Gemfibrozil is a potent inhibitor of human cytochrome P450 2C9. *Drug Metab Dispos* **29:**1359-1361.